

# Mechanical Properties of the Beetle Elytron, a Biological Composite Material

Joseph Lomakin,<sup>†</sup> Patricia A. Huber,<sup>†</sup> Christian Eichler,<sup>†</sup> Yasuyuki Arakane,<sup>‡,§</sup>  
Karl J. Kramer,<sup>‡,||</sup> Richard W. Beeman,<sup>||</sup> Michael R. Kanost,<sup>‡</sup> and Stevin H. Gehrke<sup>\*,†</sup>

Chemical and Petroleum Engineering, University of Kansas, Lawrence, Kansas 66045, United States, Department of Biochemistry, Kansas State University, Manhattan, Kansas 66506, United States, Division of Plant Biotechnology, College of Agriculture and Life Science, Chonnam National University, Gwangju 500-757, Korea, and Center for Grain and Animal Health Research, Agricultural Research Service, U.S. Department of Agriculture, Manhattan, Kansas 66502, United States

Received August 6, 2010; Revised Manuscript Received December 1, 2010

We determined the relationship between composition and mechanical properties of elytra (modified forewings that are composed primarily of highly sclerotized dorsal and less sclerotized ventral cuticles) from the beetles *Tribolium castaneum* (red flour beetle) and *Tenebrio molitor* (yellow mealworm). Elytra of both species have similar mechanical properties at comparable stages of maturation (tanning). Shortly after adult eclosion, the elytron of *Tenebrio* is ductile and soft with a Young's modulus ( $E$ ) of  $44 \pm 8$  MPa, but it becomes brittle and stiff with an  $E$  of  $2400 \pm 1100$  MPa when fully tanned. With increasing tanning, dynamic elastic moduli ( $E'$ ) increase nearly 20-fold, whereas the frequency dependence of  $E'$  diminishes. These results support the hypothesis that cuticle tanning involves cross-linking of components, while drying to minimize plasticization has a lesser impact on cuticular stiffening and frequency dependence. Suppression of the tanning enzymes laccase-2 (*TcLac2*) or aspartate 1-decarboxylase (*TcADC*) in *Tribolium* altered mechanical characteristics consistent with hypotheses that (1) ADC suppression favors formation of melanic pigment with a decrease in protein cross-linking and (2) *Lac2* suppression reduces both cuticular pigmentation and protein cross-linking.

## Introduction

**Background.** The material properties of many biological composite materials have been extensively studied, including bone, collagen, muscle, fat, cartilage, ligaments, arteries, and plant tissues.<sup>1</sup> In contrast, although insect cuticle (exoskeleton) is one of the most widespread biological composite materials found on earth, its material properties are relatively understudied. Arthropod exoskeletal material generally displays a diverse set of properties despite the fact that it is typically comprised of a limited set of organic materials, primarily the biomacromolecules chitin and protein, as well as catechols, minerals, lipids, and water. Cuticle is a lightweight, yet robust structure that allows for the sophisticated functions of flight, jumping, muscle attachment, protection, and waterproofing.<sup>2,3</sup> Within a relatively narrow density range, depending on proportions and interactions of the material components, different cuticles can display a broad range of stiffness, spanning 8 orders of magnitude in Young's modulus  $E$  (the proportionality between stress and strain).<sup>4,5</sup> The mechanical properties can vary from rigid, as is the case for a load-bearing grasshopper mandible with a Young's modulus of 15 GPa,<sup>6,7</sup> to pliant and ductile, as in the case of a locust intersegmental membrane that has a Young's modulus of only 1 kPa and a fracture strain of 150%.<sup>5,8</sup> The structural materials of other invertebrates such as the squid are comprised of similar compounds and undergo similar chemical reactions in their

development. For example, the stiffness ( $E$ ) of squid beaks varies over 100-fold from tip to base.<sup>9,10</sup>

The fact that such diverse species use similar materials and similar chemical reactions to achieve such a broad range of properties demonstrates the value of a thorough investigation of the mechanical properties of such biomaterials. Furthermore, understanding the structure–function relationships of biological materials is potentially useful for a variety of applications.<sup>11,12</sup> This work focuses on understanding how the chemical components of insect cuticle interact by examining the changes in a suite of mechanical properties as the cuticle matures in a model cuticle-rich structure, the beetle elytron or modified forewing. Beetles are studied as they comprise the dominant order of insects, they include species whose genetics and metabolism are relatively well understood, and specimens of their cuticle, such as the elytron, are easily acquired.

Insect cuticle is a complex biocomposite. Its macroscopic structure consists of an inner, pliant endocuticle, a stiff exocuticle, and an outer, waxy epicuticle.<sup>2</sup> In the forewings (elytra) of beetles, there are two layers of epidermal cells that secrete an upper and lower cuticular lamination. Between the layers is a void lamination with supporting trabeculae and hemolymph.<sup>13,14</sup> As the insect matures, the epidermal layers reduce in size, possibly fusing together, and hemolymph is resorbed. The top layer of cuticle becomes highly tanned, resulting in both pigmentation and sclerotization (hardening) of the components. The main structural components are chitin and protein. Chitin, the second most abundant biological polymer after cellulose, is arranged in microfibrils whose polysaccharide chains are hydrogen bonded to each other via the carbonyl, hydroxyl, and amino groups.<sup>15,16</sup> The fibers are usually embedded in a matrix of proteins, in layers that form a helicoidal pattern to resist

\* To whom correspondence should be addressed. Tel.: 785-864-4956. Fax: 785-864-4967. E-mail: shgehrke@ku.edu.

<sup>†</sup> University of Kansas.

<sup>‡</sup> Kansas State University.

<sup>§</sup> Chonnam National University.

<sup>||</sup> U.S. Department of Agriculture.

stresses in all directions.<sup>2</sup> Some cuticular proteins have R&R consensus sequences originally identified by Rebers and Rid-diford,<sup>17</sup> which may bind to chitin. The aromatic residues of cuticular proteins probably play a critical role in protein–protein and protein–chitin interactions.<sup>18</sup>

The basic question of whether and how chitin and protein polymeric components interact during tanning remains the subject of a more than 50-year-old debate. The quinone tanning hypothesis originally proposed by Pryor suggests that a catechol molecule can react multiple times with cuticle proteins, thereby forming an interpenetrating network (IPN) of a cross-linked protein matrix with embedded chitin fibers and pigments.<sup>19–21</sup> Specifically, catechols produced by metabolism of tyrosine and L-aspartic acid are oxidized by the phenoloxidase laccase2 (Lac2) to generate *o*-quinone or *p*-quinone methide derivatives. These electrophiles in turn are believed to be responsible for producing polymeric pigments and for cross-linking cuticular proteins. A possible cross-linking pathway, in which histidyl residues in cuticular proteins serve as nucleophiles that undergo Michael addition reactions with the quinones, has been proposed.<sup>22</sup> Such a mechanism also suggests the possibility of catechol-mediated cross-links with glucosamine residues of deacetylated chitin.<sup>23–25</sup> Unfortunately, while protein–catechol adducts have been identified, the formation of cross-links with the proteins and polysaccharide has been difficult to confirm by standard biochemical methods, such as mass spectrometry of cuticle degradation products.<sup>26</sup> However, the analogous chemistry in sclerotized squid beaks was recently confirmed, where histidine residues on cuticle proteins become linked via quinones derived from 4-methylcatechol or L-3,4-dihydroxyphenylalanine (DOPA).<sup>10</sup>

Quinone tanning reactions increase the hydrophobicity of the cuticle, which, when combined with overall dehydration upon ecdysis, results in a decreased water content as tanning proceeds. The leading alternative explanation for the sclerotization of cuticle is that loss of water alone is sufficient to explain its hardening. The hypothesis is that hardening is due to a combination of increased hydrogen bonding among the macromolecular components and the loss of plasticization by water upon drying.<sup>27,28</sup> In one argument supporting this view and opposing the quinone tanning hypothesis, Vincent has recently reasoned that because cuticle can swell in a hydrogen bond-breaking solvent,<sup>29</sup> covalent cross-links must not exist to the extent necessary to account for the mechanical property changes upon tanning.<sup>28</sup> However, it is well established theoretically and experimentally that swelling of networks in solvents is the result of a balance between cross-link density and polymer–solvent interaction as well as charge density of polyelectrolyte networks.<sup>30</sup> Thus, changing solvent quality will induce changes in swelling of any elastic network, without requiring any changes in cross-link density (in mol/cm<sup>3</sup> polymer) or average molecular weight between cross-links in order to do so.<sup>31</sup> Hence, the observation of changes in cuticle swelling upon changes in solvent does not resolve this debate.

Nonetheless, it is likely that noncovalent interactions among macromolecular components of the cuticle do contribute to its mechanical properties, but it is also likely that covalent cross-links strengthen the cuticle as well. The question, then, is one of the relative importance of each of the two contributors. Recently, it was shown using NMR spectroscopy that gelatin reacts with phenolic compounds to form C–N covalent bonds, leading to decreased molecular mobility and maintenance of a high modulus even at high temperatures.<sup>32</sup> However, because tanning reactions and dehydration happen simultaneously, it has

been unclear whether the change in mechanical properties during tanning results mainly from covalent cross-linking or the effects of dehydration. Similar to the case of insect cuticle, a recent report on the tanning of the squid beak suggests the existence of catechol–protein cross-links and possibly chitin–protein cross-links, but the authors explicitly note that they could not resolve the respective contributions of cross-linking and dehydration in that tissue.<sup>9</sup> In that report, it was the spatial gradients in tanning that were examined, while in this work on insect cuticle, it is the temporal changes in tanning which are examined as the insect matures. Another report discussing the effects of water on the mechanical properties of cellulose also emphasizes the importance of understanding the structural origin of mechanical properties.<sup>33</sup> Vincent notes the need to combine biochemical and mechanical techniques in order to resolve these questions,<sup>28</sup> and that is the approach we have taken in this work.

**Objectives.** In this work, the nature of intermolecular interactions in the cuticle of the elytron has been examined using a combination of biochemical and mechanical approaches. With a purely biochemical approach, it is difficult to ascertain molecular interactions due to the inextractable nature of the components of the exoskeleton. Even exposure to harsh chemical conditions such as boiling in the presence of a strong base or acid has yielded only a partial recovery of cuticular components.<sup>34,35</sup> Furthermore, such extractions become increasingly ineffective as the cuticle tans, and the degradation associated with these extraction methods makes it impossible to recover components in their native biological form. Thus, we have used dynamic mechanical analysis and RNA interference (RNAi) to probe the underlying molecular interactions among cuticular components in a bulk cuticle-rich structure, the beetle elytron.

The present study is based on the hypothesis that cuticle structure, made from a limited set of polymeric materials, is amenable to modeling using the methods of physical polymer science. Dynamic mechanical analysis is a common way to evaluate the contribution of cross-linking in synthetic polymeric materials, including composites. We have recently applied this technique to a study of a complex mammalian tissue, the temporomandibular joint disk.<sup>36</sup> In particular, frequency sweeps are an effective method for measuring the development of cross-links, entanglements, and other interactions within synthetic and natural gelling systems.<sup>37–44</sup> The cross-linking of polymers leads to an increase in the elastic response relative to the viscous response to applied stress. Because elasticity is independent of strain rate, the moduli of more highly cross-linked materials are less dependent on oscillation frequency than are less cross-linked materials. Thus, this technique is applied here as a means to evaluate the presence of cross-linking in the elytral cuticle, to correlate the extent of cross-linking with cuticle tanning and to separate the relative importance of cross-linking versus loss of plasticization upon dehydration in the development of the mechanical properties of the mature elytron.

The relatively rectangular shape of the elytron offers a convenient sample for mechanical analysis and requires minimal preparation for study. Therefore, we determined a comprehensive set of material properties for elytra from two agricultural pest insects in the beetle family Tenebrionidae, namely, the red flour beetle, *Tribolium castaneum*, and the yellow mealworm, *Tenebrio molitor* (hereafter referred to as simply *Tribolium* and *Tenebrio*, respectively). *Tenebrio* was chosen due to its relatively large size, which made the elytral samples easier to manipulate. *Tribolium* was selected because its genome has been sequenced,<sup>45</sup> its developmental stages are regular and easily observable, and it was possible to experimentally modulate the

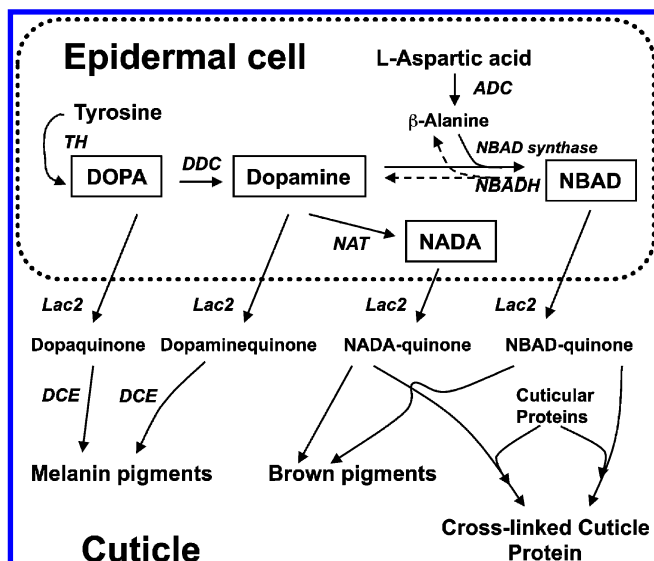


**Figure 1.** Proposed cuticle tanning metabolic pathway in *Tribolium castaneum* and *Tenebrio molitor*. TH = tyrosine hydroxylase, DOPA = 3,4-dihydroxyphenylalanine, Dopamine = 3,4-dihydroxyphenethylamine, DDC = dopa decarboxylase, NADA = *N*-acetyldopamine, NBAD = *N*- $\beta$ -alanyldopamine, ADC = aspartate 1-decarboxylase, NBADH = *N*- $\beta$ -alanyldopamine hydrolase, DCE = dopachrome conversion enzyme, and Lac2 = laccase 2.

levels of tanning enzymes in *Tribolium* by utilizing RNAi.<sup>46,47</sup> In addition, several tanning metabolic enzymes shown in Figure 1 and their impact on cuticle properties have been the subject of a recent study.<sup>48</sup>

We have shown that relevant mRNA and protein levels can be systematically manipulated in *Tribolium* by the RNAi technique.<sup>49</sup> In the present study, the two enzymes shown in Figure 1 targeted for down-regulation by this method are laccase 2 (*TcLac2*) and aspartate 1-decarboxylase (*TcADC*). Based on the proposed cuticular metabolism, it is hypothesized that knockdown of *TcLac2* activity will limit the formation of melanic pigment polymers and also decrease the levels of cuticle protein cross-linking agents. Down-regulation of ADC transcripts will reduce the synthesis of  $\beta$ -alanine used for production of *N*- $\beta$ -alanyldopamine (NBAD), a major cross-linking agent precursor. The reduced availability of NBAD due to ADC suppression is hypothesized to promote the development of melanic pigments at the expense of protein cross-linking because the catechol normally involved in cross-linking will instead follow the metabolic pathway toward the formation of melanin pigments.<sup>48</sup> This RNAi approach holds promise for systematic variation of chemical composition of many types of biosynthetic materials and also the extent of cross-linking.

Our comprehensive examination of elytral mechanical performance as a function of multiple variables aims to shed light on the roles and interactions of the primary cuticle components including protein, catechol, chitin and water. The self-reinforcing data obtained provide support for the importance of cross-link formation on elytral physical behavior. Such analysis may be useful as a means of assessing microstructural organization in other biological materials as well. Furthermore, we used RNAi to test hypotheses suggested by the metabolic pathways involved in tanning, which are shown in Figure 1.

## Experimental Section

**Materials.** Elytra from *Tribolium castaneum* (GA1 strain) and *Tenebrio molitor* were used in the experiments. To evaluate the effect

of gene suppression on mechanical properties, double stranded RNAs (dsRNA) for *Tribolium* laccase 2 (*dsTcLac2*, 2 ng per insect) or aspartate decarboxylase (*dsTcADC*, 200 ng per insect) were prepared and injected into the dorsal abdomen of pharate pupae or 1–2 d old pupae, as described elsewhere.<sup>49,50</sup>

Insects were reared at the ARS-USDA Center for Grain and Animal Health Research in Manhattan, KS, under standard conditions, *Tribolium* on a diet of wheat flour fortified with 5% brewers' yeast and *Tenebrio* on the same diet supplemented with an equal volume of rolled oats. Pupae were shipped overnight in capped vials to the University of Kansas, where they were allowed to mature into adults, from which elytra were removed and tested at the appropriate tanning state. Untanned and partially tanned (24 h of tanning) elytra contain a significant amount of water, and thus, these were harvested and tested immediately to minimize water loss prior to measurement. Elytra were also dried in a desiccator over calcium sulfate. Elytra from beetles that had been prevented from undergoing the natural tanning process by injections of *dsTcLac2* or *dsTcADC* were harvested and prepared in a similar manner.

**Methods.** A TA Instruments RSAIII dynamic mechanical analyzer was used to perform all of the mechanical measurements. The instrument utilizes a separate direct drive linear motor to apply a strain and force transducer to measure the resulting force.<sup>51</sup> This combination accounts for the high force resolution of the instrument, down to  $10^{-4}$  N, and a strain resolution down to 1 nm, capabilities which were necessary to obtain reproducible results on these small specimens. The frequency range of  $10^{-1}$  to 600 rad/s was used for dynamic mechanical analysis.

Prior to mechanical testing, the beetles were sacrificed by exposure to  $-20$  °C for 30 min (no significant differences in static or dynamic mechanical tests were observed in comparison to elytra removed from live insects). Elytra were removed with tweezers and immediately tested. Several mounting techniques were employed for sample measurements. Soft samples were gripped directly between the instrument's metal clamps. Harder, brittle samples such as dried and tanned *Tribolium* elytra required strips of plastic to be clamped in the mounts with epoxy used to attach the samples to the strips. Devcon 1.5 ton quick-setting epoxy cement was allowed to dry for 1 h prior to testing; fixing such samples without damage was confirmed optically and by reproducibility of results. The epoxy was confirmed stiff enough not to compromise results by comparison with results obtained from mounting and testing in a comparable fashion plastic and aluminum strips of known properties. Sample dimensions were determined via calipers and microscopic measurements utilizing a digital micrometer. The elytra were tested whole, without being cut into a particular test shape beforehand. Geometric uniformity was assured by clamping such that a rectangular portion of the elytron remained between the grips. The length and width of the rectangular portion of elytra after mounting for mechanical tests were  $1 \times 0.8$  mm for *Tribolium* and  $3-4 \times 2.8-3$  mm for *Tenebrio*.

Once the samples were mounted, ultimate properties were determined via static stress–strain measurements. All ultimate property measurements were made under extension. The extension rate was set to 0.01 mm/s to allow for sufficient data collection quickly enough so that drying was minimized during the test. The calculations used an engineering stress based on the initial cross-sectional area of the sample, approximated as the product of the elytron's centerline width (measured by calipers to be nearly constant within  $\pm 20\%$ ) and its centerline thickness (measured under an optical microscope with a digital filar micrometer). It was not feasible to measure the exact dimension of each sample tested, so the average cross-sectional area of a population was used in stress calculations as summarized in Table 1a,b. The dimensions obtained by these measurement methods were confirmed by scanning electron microscopy. Elytra were collected from the adults using a forceps at approximately 1, 24, and 168 h posteclosion and then immediately frozen in liquid nitrogen. Frozen elytra were fractured and prepared for SEM at the Kansas State University Scanning Electron



Table 1<sup>a</sup>

(a) Physical Properties of <i>Tribolium</i> Elytra				
elytral sample	thickness by freeze-fracture SEM ( $\mu\text{m}$ )	thickness by optical microscopy ( $\mu\text{m}$ )	$L/L_0$ (thickness/untanned thickness)	water content (g/g)
untanned	10–12	$14 \pm 2$	1	$0.66 \pm 0.06$
partially tanned (24 h)	15–18	$16 \pm 5$	$1.2 \pm 0.3$	n/a
fully tanned (7 d)	25–30	$25 \pm 3$	$1.8 \pm 0.2$	$0.26 \pm 0.04$
ds <i>TcLac2</i> -treated (72 h)	n/a	$22 \pm 3$	$1.6 \pm 0.2$	n/a
Properties after Drying				
untanned	n/a	$9 \pm 2$	$0.6 \pm 0.3$	$0.02 \pm 0.01$
fully tanned (7 d)	n/a	$21 \pm 3$	$1.5 \pm 0.2$	$0.01 \pm 0.01$
(b) Physical Properties of <i>Tenebrio</i> Elytra				
elytral sample	thickness by freeze-fracture SEM ( $\mu\text{m}$ )	thickness by optical microscopy ( $\mu\text{m}$ )	$L/L_0$ (thickness/untanned thickness)	water content (g/g)
untanned	12–14	$14 \pm 2$	1	$0.71 \pm 0.05$
partially tanned (24 h)	17–20	$18 \pm 3$	$1.3 \pm 0.2$	n/a
fully tanned (7 d)	55–66	$51 \pm 8$	$3.6 \pm 0.2$	$0.33 \pm 0.05$
Properties after Drying				
untanned	n/a	$9 \pm 2$	$0.6 \pm 0.3$	$0.02 \pm 0.01$
fully tanned (7 d)	n/a	$39 \pm 7$	$2.7 \pm 0.2$	$0.01 \pm 0.01$

<sup>a</sup>  $\pm 95\%$  confidence intervals,  $n = 6$  except for untanned elytra where  $n = 10$ . SEM data is observed range.

Microscope Laboratory. The thickness values of *Tribolium* untanned, partially tanned, and fully tanned elytra obtained from the light microscopic observations without freezing matched those obtained by SEM measurements (Table 1a,b).

Dynamic experiments included strain sweeps and frequency sweeps. For strain sweeps, a frequency of 6.28 rad/s (1.0 Hz) was selected. The strain-independent linear viscoelastic region determined by strain sweeps was maintained past a strain of 0.1% for all of the elytron types tested; thus, a strain of 0.1% was used for all frequency sweep experiments. Frequency sweeps were performed from 0.1 to 600 rad/s to measure the elastic (storage) modulus  $E'$ , the viscous (loss) modulus  $E''$ , and their ratio  $E''/E'$ , which is also known as  $\tan \delta$ . The variation of the elastic modulus  $E'$  with strain wave oscillation frequency was fit to a power law model ( $r^2 > 0.95$ ) between 10 and 100 rad/s.

It was important that fresh elytra be tested quickly because they can lose a significant amount of water to the atmosphere, which impacts their mechanical properties. Mounting of elytra immediately after harvesting ensured that no more than 3% of the total mass and no more than 15% of the water were lost prior to measurement, as confirmed by gravimetric analysis using TA Instruments TGA/DSC Model Q600 ( $\pm 1 \mu\text{g}$ ). To prepare dried samples for mechanical measurements, elytra were placed in a calcium sulfate desiccator at room temperature for at least 24 h prior to mounting until a constant mass was reached, which was confirmed by using a sufficient mass of elytra to be measured accurately with an analytical balance ( $\pm 0.1 \text{ mg}$ ).

The water content of desiccator-dried and freshly harvested untanned and fully tanned elytra was determined by thermogravimetric analysis under dry nitrogen gas at 30 °C. In dry nitrogen at 30 °C, the tanned elytra lose  $\sim 3 \text{ wt } \%$  during the first 1.5 h. Both tanned and untanned *Tribolium* and *Tenebrio* elytra dry to a constant mass over 24 h at room temperature and over 3 h at 100 °C. These data confirmed the mass measurements determined by using an analytical balance and the dimensional measurements as described above.

## Results

The results will be presented in three parts: macroscopic characterization, static mechanical analysis, and dynamic mechanical analysis. Elytra are not entirely homogeneous, as observed by stereomicroscopy and scanning electron microscopy. Most notably, the dorsal side of the elytra reveals ribs

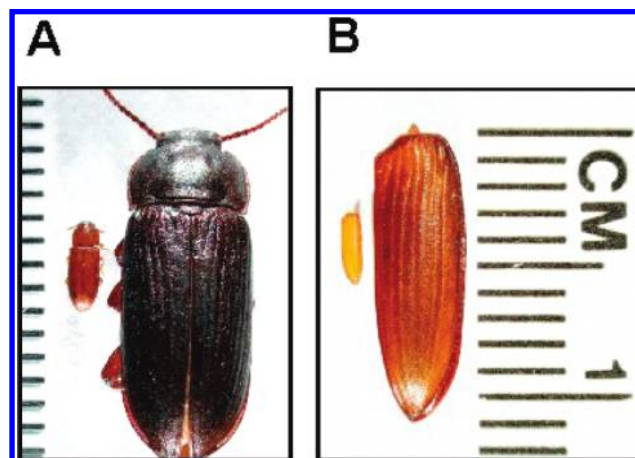


**Figure 2.** Two coleopteran species and their elytra used in this study. (A) Adults of *Tribolium castaneum* (left) and *Tenebrio molitor* (right). (B) Elytra (modified and highly tanned forewings) from the same. Scale bars are in mm.

that apparently provide additional structural support. In static tests these ribs are visibly responsible for stopping propagation of cracks, most notably in partially tanned elytra. Due to sample heterogeneity and small size, 95% confidence intervals of moduli, especially those where sample size was limited, can be large. However, for dimensionless properties such as  $E''/E'$ , confidence intervals are typically on the order of 10% of the mean. Such variability is not unusual for biological systems and does not obscure the clear trends that are described below.

**Macroscopic Characterization.** When viewed under a stereomicroscope, *Tribolium* and *Tenebrio* elytra are geometrically similar but differ in size and color, as shown in Figure 2. The color of a *Tenebrio* elytron is darker than that of *Tribolium*.<sup>52</sup> Both species require from 4 to 7 days posteclosion to reach a fully tanned state under our rearing conditions.<sup>53,54</sup> This observation is based on the fact that little or no changes in coloration, cuticle thickness, or mechanical properties are observed past this time. For both species, as tanning proceeds, cuticle thickness and water content change substantially. Table 1 reports these changes for untanned (measured within ap-

Table 2<sup>a</sup>

(a) Static Mechanical Properties of <i>Tribolium</i> elytra						
elytral sample	number of samples	Young's modulus (MPa)	fracture strain (%)	fracture stress (MPa)	toughness (work to fracture; MPa)	
untanned	5	37 ± 16	12 ± 3.2	3.9 ± 0.5	0.2 ± 0.1	
partially tanned (24 h)	5	210 ± 60	4.6 ± 0.7 (initial) 10.0 ± 2.0 (maximum)	5.8 ± 0.6 (initial) 10.1 ± 5.1 (maximum)	0.4 ± 0.1	
dsTcLac2-treated (72 h)	2	230 ± 220	3.7 ± 2.1	3.6 ± 0.8	0.1 ± 0.1	
(b) Static Mechanical Properties of <i>Tenebrio</i> elytra <sup>a</sup>						
elytral sample	number of samples	Young's modulus (MPa)	fracture strain (%)	fracture stress (MPa)	toughness (work to fracture; MPa)	
untanned	5	51 ± 12	10.0 ± 0.9	6.1 ± 1.6	0.3 ± 0.1	
partially tanned (24 h)	4	320 ± 140	3.1 ± 0.9 (initial) 5.1 ± 0.7 (maximum)	11.9 ± 3.5 (initial) 14.7 ± 7.0 (maximum)	0.4 ± 0.2	
fully tanned (~7 d)	6	1000 ± 210	3.1 ± 1.1	29.0 ± 4.1	0.5 ± 0.2	
fully tanned (~7 d), dry	4	2300 ± 810	3.0 ± 0.6	67 ± 23	1.0 ± 0.5	

<sup>a</sup> ±95% confidence intervals.

proximately 1 h after eclosion), partially tanned (measured approximately 24 h after eclosion), and fully tanned (measured at least 7 days after eclosion) elytra. Water content for elytra at different stages was determined via mass change upon drying in the presence of dry nitrogen gas at 30 °C. Such measurements utilized multiple elytra simultaneously and yielded comparable results, ~70% water content for an untanned elytron and ~30% for a fully tanned elytron (Table 1). The elytron loses a large fraction of this water during the course of the tanning process and the thickness more than doubles, presumably through the addition of cuticular material added from underlying epidermal cells. The *Tenebrio* elytron thickens substantially more than *Tribolium*, but the relative contributions of each component to the thickening and density differences are unknown. Nonetheless, the general progress of dehydration and increase in nonvolatile mass holds true for both *Tribolium* and *Tenebrio* elytra.

Optical thickness measurements were confirmed by scanning electron micrographs of freeze-fractured elytra. The thickness of a *Tribolium* elytron increases about 2-fold during maturation from ~10 to 20 μm. Most of this increase is due to the development of trabecula (beam-like structures) within the dorsal and ventral layers. The ventral layer has little pigmentation; it is primarily the dorsal layer that tans.

**Static Mechanical Analysis.** The elytral properties measured in static mechanical analysis are summarized in Table 2. These properties are obtained from stress–strain curves of which representative examples for different freshly harvested elytra are shown in Figures 3–6. The data provide a detailed view of the stress–strain behavior of the elytra and the range of experimental variability observed.

**Effects of Tanning on Static Properties.** Fully tanned elytra behave as brittle plastics, with a linear stress–strain curve followed by abrupt fracture occasionally interrupted by rib structures. (Figure 3).<sup>55</sup> In contrast, untanned and partially tanned elytra are relatively ductile, behaving as soft but tough plastics. Such samples also exhibit piece-by-piece tearing of the sample, with cracks interrupted by ribs in the elytra without a complete fracture (Figures 4–6). For partially tanned elytra, stress–strain curves typically exhibit local maxima or plateaus before reaching the global maximum, whereas for untanned elytra stress declines steadily and irregularly as it tears.<sup>56</sup>

Figure 3 displays the stress–strain behavior of fully tanned *Tenebrio* elytra. The average fracture stress of the elytra is 29.0 ± 4.1 MPa, a fracture strain of 3.1 ± 1.1%, and a Young's

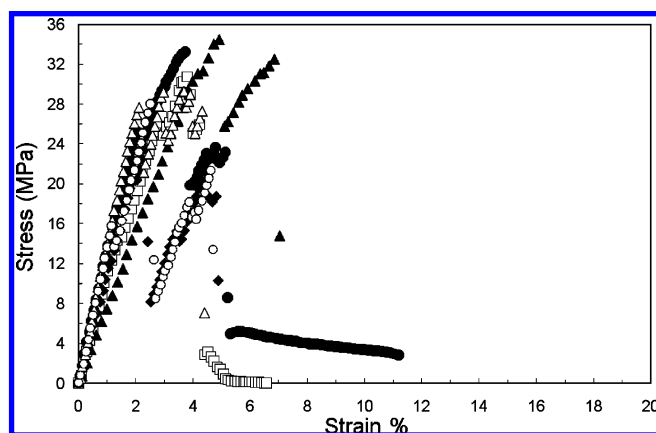


**Figure 3.** Six representative stress–strain curves for fully tanned *Tenebrio* elytra. The failure is more abrupt in brittle, fully tanned elytra than in untanned elytra.

modulus ( $E$ ) of 1000 ± 210 MPa. The large standard deviations are typical of fracture tests of this type, amplified by the small size and slight curvature of the elytra. These values are comparable to synthetic engineering plastics such as polystyrene and epoxy resins.<sup>57</sup> Qualitatively, the ultimate properties of fully tanned *Tribolium* and *Tenebrio* elytra appear similar. Unfortunately, the stiffness, brittleness, and small size of fully tanned *Tribolium* elytra meant that only semiquantitative results could be obtained for those samples.

The stress–strain results obtained for untanned *Tribolium* and *Tenebrio* elytra are shown in Figure 4a and b, respectively. The material response of untanned cuticle is also largely linear up to the failure point with an  $E$  value of 37 ± 16 MPa, a fracture stress of 3.9 ± 0.5 MPa, and a fracture strain of 12.0 ± 3.2% for *Tribolium* and an  $E$  value of 51 ± 12 MPa, an average fracture stress of 6.1 ± 1.6 MPa, and a fracture strain of 10.0 ± 0.9% for *Tenebrio*. Thus, for both species, tanning increases  $E$  about 20 times, while the fracture strain drops by a factor of 3. Notably, the failure is not complete at the point of initial fracture; instead, piecewise tearing of the samples leads to an irregular decline of the stress as strain is increased. The decline in modulus is associated with the irregular manner in which tears are propagated. The measure of toughness known as “work to fracture” reported here uses only the area up to the point of tearing. It is observed that after the initial fracture, the crack will grow quickly upon increasing strain until encountering a rib. The rib arrests crack propagation until it also fails, with

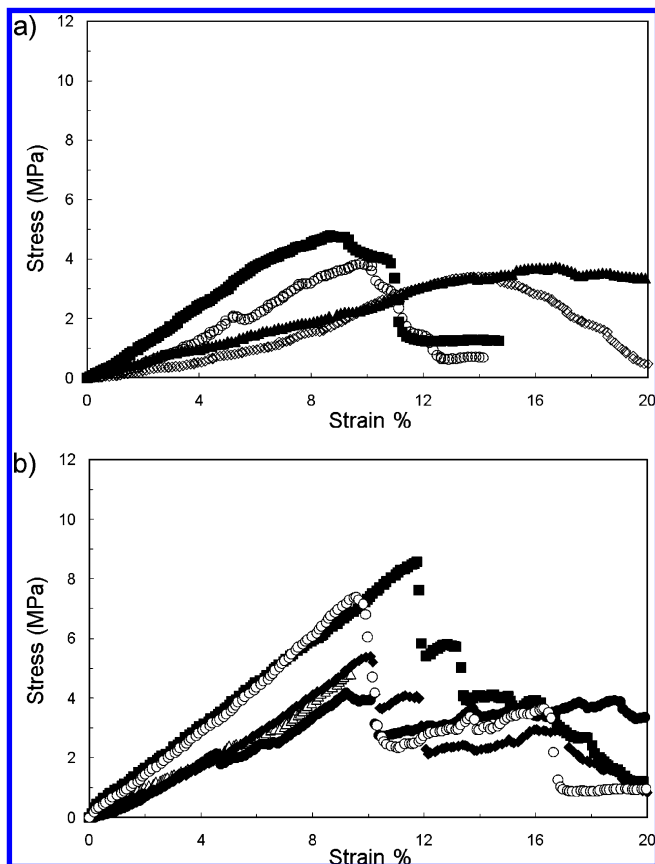


**Figure 4.** Four representative stress–strain curves for (a) untailed *Tribolium* elytra and (b) untailed *Tenebrio* elytra. The untailed elytra are softer and more ductile than fully tanned elytra and tear rather than abruptly fracture. Force–strain data past point of initial fracture were not used in calculations because substantial irregular tearing renders stress calculation meaningless.

this process repeating until complete failure occurs. The piecewise tearing is more pronounced in elytra allowed to tan for 24 h, as shown in Figure 5a and b. In partially tanned elytra distinct fracture points are visible prior to reaching the maximum failure stress. The Young's modulus calculated both before and after this initial fracture stress remained nearly constant despite the primary material failure as indicated by a sharp temporary decline in the stress–strain curve. This behavior indicates that the cuticle properties between the ribs are uniform across the structure. It also suggests that the cuticle within the ribs may tan faster than the cuticle between the ribs, reaching uniform properties upon maturity. The fracture properties of this material were calculated both at the initial fracture and also at the highest achieved fracture stress and its corresponding strain. *Tribolium* elytra that have undergone tanning for 24 h exhibit a maximum fracture stress of  $10.1 \pm 5.1$  MPa, a fracture strain of  $10.0 \pm 2.0\%$  and an  $E$  value of  $210 \pm 60$  MPa. *Tenebrio* elytra that have undergone tanning for 24 h exhibit a maximum fracture stress of  $14.7 \pm 7.0$  MPa, a fracture strain of  $5.1 \pm 0.7\%$  and an  $E$  value of  $320 \pm 140$  MPa. While these data indicate that the elytra have become significantly stiffer during the first 24 h after eclosion, they are still nearly three times weaker than when they become fully tanned several days later.

**Effects of Laccase Suppression on Static Properties.** Lastly, the ultimate properties of *TcLac2*-suppressed *Tribolium* elytra were tested. When *TcLac2* transcript levels were substantially reduced by injection of *TcLac2* dsRNA (200 ng per insect), the pupae could not molt to the adult and subsequently died.<sup>49</sup> Hence, the tested samples were derived from insects injected

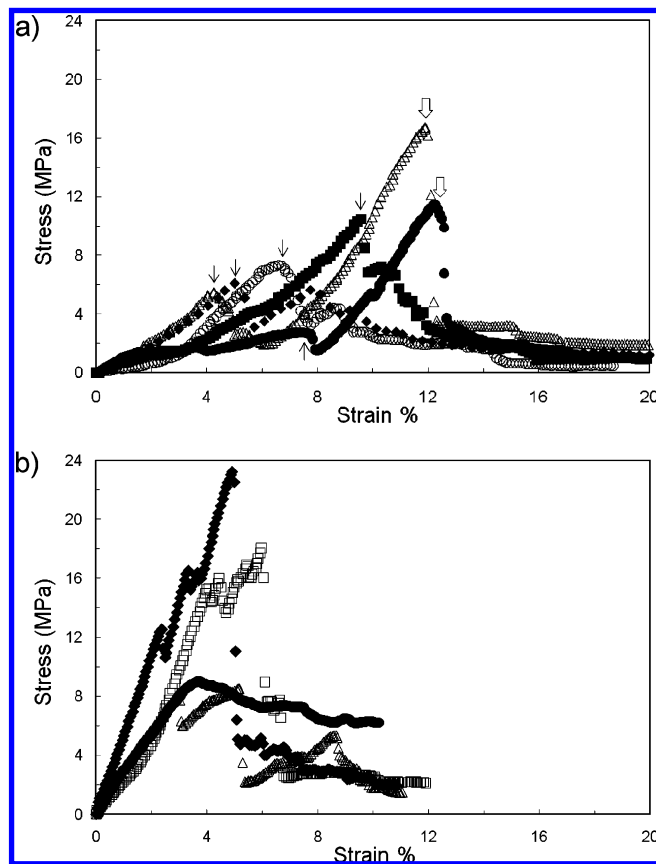


**Figure 5.** Four representative stress–strain curves for (a) *Tribolium* elytra and (b) *Tenebrio* elytra that have undergone approximately 24 h of tanning. The behavior shows pronounced irregular tearing. Small arrows correspond to primary fracture points and large arrows to global maxima.

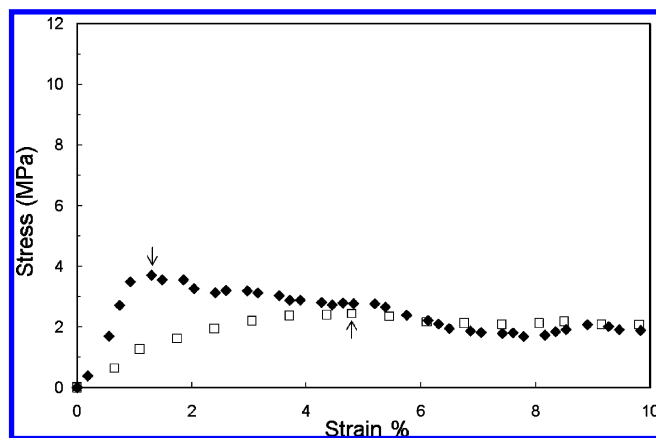


**Figure 6.** Two representative stress–strain curves for laccase-suppressed *Tribolium* elytra that had undergone tanning for 3 d. Arrows correspond to primary fracture points. Behavior is comparable to normal elytra that have tanned for 24 h, up to about 5% strain.

with a lower dose of dsRNA for this gene (2 ng per insect), one that does not prevent adult eclosion. Under these conditions some tanning clearly occurs as the exoskeleton turns a very light brown color. Nonetheless, the *TcLac2*-suppressed beetles were unable to complete the tanning process and died prematurely. After approximately 3 days, elytra from ds*TcLac2*-treated insects were harvested for testing. Figure 6 shows the stress–strain response for these elytra; the response was initially linear before fracturing at a global maximum, followed by a steady tearing. The average fracture stress was  $3.6 \pm 0.8$  MPa with a fracture strain of  $3.7 \pm 2.1\%$ .



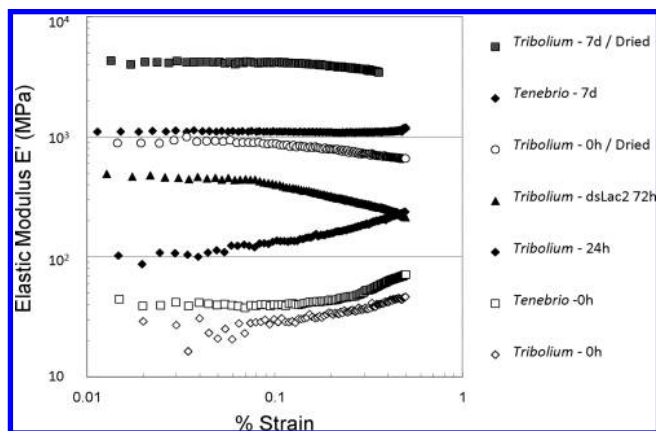


**Figure 7.** Representative strain sweeps of various elytral samples at 6.28 rad/s (1.0 Hz). Elytra show stable linear viscoelastic behavior up to 0.1% strain. Data are truncated above 0.5% as samples begin to break down above this value.

Notably, the *dsTcLac2* elytra are weak and only 5 times stiffer ( $E = 230 \pm 220$  MPa) than untanned elytra. The water content was somewhat less than that of untanned elytra but was still on the order of 50%. The increased strength must therefore be attributed to compositional changes beyond dehydration. Overall, the static properties of *dsTcLac2* elytra are similar to those of partially (24 h) tanned elytra. That is, stiffness of laccase-deficient cuticle at 3 d is similar to the stiffness of normal cuticle at 1 d (see the primary fracture points in Figures 5a and 6). However, *dsTcLac2* elytra have inferior global fracture properties and do not exhibit the piecemeal tearing pronounced in wild-type partially tanned elytra while fracturing abruptly. Clearly, a significant component of the tanning process was disrupted by injection of *dsTcLac2*.

**Dynamic Mechanical Analysis.** Dynamic mechanical analysis yields information that is helpful for understanding the interactions of the different components in the elytron. Strain sweep experiments at 6.28 rad/s (1.0 Hz) were performed first to establish the linear viscoelastic region of the various types of elytra tested. Representative strain sweep data are shown in Figure 7 and the summary of those experiments is presented in Table 3a,b. At strains below 0.1%, all of the elytra exhibited strain-independence. Hence, 0.1% was the strain value chosen for all subsequent frequency sweeps. In some cases at strains above  $\sim 0.5\%$ , the elastic modulus of the elytra becomes a strong function of the strain and at strains above 1%, the elytra eventually fail (data at high strain values not shown). Additional information about structure can be gathered from the dynamic frequency response of the elytron.

**Effects of Tanning on the Dynamic Modulus.** From Figures 8a and 9a, it is evident that the elytra of *Tribolium* and *Tenebrio* immediately after eclosion are quite weak as indicated by elastic modulus ( $E'$ ) values at 6.28 rad/s of  $60 \pm 7$  and  $52 \pm 13$  MPa, respectively. As the elytra tan, their stiffness increases due to tanning reactions and water loss. To study the relative significance of each of these processes, frequency sweeps on elytra at various tanning stages and hydration levels were performed (hydration data shown in Table 1). A comparison of Tables 2 and 3 illustrates that  $E'$  values measured in either strain sweep or frequency sweep experiments at 1 Hz are comparable in magnitude to  $E$ , as expected ( $E = [E'^2 + E''^2]^{1/2}$  at a given frequency and  $E' \gg E''$  in all cases).  $E'$  exhibits the same dramatic increase as a function of tanning time as the  $E$  obtained from static tests. For *Tenebrio*, upon full tanning the modulus increases  $20 \pm 6$  times in  $E$ ,  $28 \pm 7$  times in  $E'$  (strain sweep),

and  $20 \pm 6$  times in  $E'$  (frequency sweep). For fully tanned *Tribolium* elytra, the modulus increases are comparable,  $43 \pm 9$  times in  $E'$  (strain sweep) and  $20 \pm 3$  times in  $E'$  (frequency sweep). The 24 h tanned *Tenebrio* elytra exhibit modulus increases of  $6 \pm 4$  in  $E$  and  $4 \pm 1$  in  $E'$  measured by strain and  $10 \pm 4$  in frequency sweeps. Partially tanned *Tribolium* elytra show an increase of  $6 \pm 3$  in  $E$  and  $5 \pm 2$  in  $E'$  measured by strain and  $4 \pm 2$  in frequency sweeps. The tables show that the moduli of *Tenebrio* and *Tribolium* are comparable in magnitude, while the tanning process stiffens elytra from both species over 20 times.

**Effects of Drying on the Dynamic Modulus.** Drying an untanned *Tribolium* elytron, which is  $66 \pm 6\%$  water, increases its elastic modulus  $18 \pm 2$  times, but the increase is only  $7 \pm 1$  times for *Tenebrio*. Thus, while drying increases the modulus significantly, tanning has the greater effect. Comparing elytra in their dried state before and after tanning suggests that tanning accounts for an additional  $4 \pm 1$ -fold increase in stiffness for *Tribolium* and  $5 \pm 2$ -fold increase in stiffness for *Tenebrio*. These trends are more clearly seen by examining the entire frequency sweep curves for the elytra in Figures 8a and 9a.

**Effects of RNAi on the Dynamic Modulus.** Additionally, disruption of the insect's catechol metabolism by injection of dsRNAs has very different effects depending upon the gene targeted by dsRNA. After injection of *TcLac2* dsRNA, which suppresses *TcLac2* transcripts and subsequent oxidation of catechols to form quinones that can polymerize or form cross-links, a weakened hydrated elytron is obtained, with a modulus of only about 200 MPa. This represents an increase of less than 1 order of magnitude from the untanned state. In contrast, knock down of *TcADC* transcripts, which should disrupt synthesis of  $\beta$ -alanine required to synthesize the cross-linking agent precursor *N*- $\beta$ -alanyldopamine (NBAD), more than doubles the modulus ( $2.6 \pm 0.3$ -fold increase), as shown in Figure 9.

**Trends in the Frequency Exponent and  $\tan \delta$ .** The elastic modulus of all of the elytra tested was frequency dependent, as shown in Figures 8a and 9a. This dependence was fit to a power law model over the range 10–100 rad/s, the exponent of which was used as a measure of elytral component interactions, as discussed in the next section. These exponents are summarized in Table 3 and presented in Figure 10 to illustrate the trends with tanning time and drying for both species. The two coleopteran species show the same trends in the exponent as a function of tanning and drying. The highest values of the power law exponent are seen for the untanned and hydrated cuticle with values of  $0.095 \pm 0.012$  and  $0.130 \pm 0.037$  for *Tribolium* and *Tenebrio* elytra, respectively. Drying the elytron decreased the power law dependence to  $0.069 \pm 0.015$  and  $0.040 \pm 0.005$ , respectively. Tanning and drying reduced the power law dependence even further to  $0.025 \pm 0.001$  and  $0.018 \pm 0.001$ , respectively.

The frequency dependence of the elastic modulus of *Tribolium* elytra was also determined after RNAi treatment. *dsTcLac2* elytra exhibited a low  $E'$  frequency dependence comparable to that of fully tanned elytra, suggesting that despite a reduction in *TcLac2* transcripts, some tanning had taken place (because only a partial knockdown of transcripts had occurred so as to permit adult eclosion) as the static data also supported. Conversely, the frequency dependence of the elastic modulus of fully tanned *dsTcADC* elytra was higher than that of normal fully tanned elytra, showing that down-regulation of *TcADC* transcripts also alters elytral properties but much differently from down-regulation of *TcLac2*. Because the power law exponent is independent of dimensional measurements, uncertainty in this

Table 3<sup>a</sup>

(a) Dynamic Mechanical Properties of <i>Tribolium elytra</i>							
elytral sample	No.	strain sweep @ 1 Hz		frequency sweep @ 0.1%			
		$E'$ @ 0.1% (MPa)	linear viscoelastic range	No.	$E'$ @ 1 Hz (MPa)	$E''/E'$ @ 1 rad/s	frequency power law exponent
untanned	2	30 ± 6	0.01–0.4	6	60 ± 7	0.21 ± 0.03	0.095 ± 0.012
partially tanned (24 h)	3	140 ± 40	0.01–0.2	4	240 ± 150	0.13 ± 0.03	0.082 ± 0.012
fully tanned (7 d)	2	1300 ± 100	0.01–0.3	6	1200 ± 100	0.08 ± 0.02	0.035 ± 0.003
ds <i>TcLac2</i> -treated (72 h)	2	350 ± 50	0.01–0.2	3	230 ± 140	0.18 ± 0.02	0.043 ± 0.005
ds <i>TcADC</i> -treated (7 d)	3	3200 ± 400	0.01–0.2	4	3100 ± 300	0.20 ± 0.03	0.062 ± 0.006
Properties after Drying							
untanned	1	880	0.01–0.7	3	1100 ± 100	0.17 ± 0.03	0.069 ± 0.015
fully tanned (7 d)	1	4200	0.01–0.4	6	4000 ± 800	0.07 ± 0.02	0.025 ± 0.001
ds <i>TcADC</i> -treated (7 d)	1	3600	0.01–0.1	4	3500 ± 600	0.14 ± 0.02	0.038 ± 0.002
(b) Dynamic Mechanical Properties of <i>Tenebrio elytra</i>							
elytral sample	No.	strain sweep @ 1 Hz		frequency sweep @ 0.1%			
		$E'$ @ 0.1% (MPa)	linear viscoelastic range	No.	$E'$ @ 1 Hz (MPa)	$E''/E'$ @ 1 rad/s	frequency power law exponent
untanned	1	40	0.01–0.2	3	52 ± 13	0.24 ± 0.03	0.130 ± 0.037
partially tanned (24 h)	1	440	0.01–0.2	3	540 ± 220	0.11 ± 0.02	0.035 ± 0.001
Fully tanned (7 d)	3	1100 ± 260	0.01–0.4	6	1020 ± 200	0.07 ± 0.01	0.021 ± 0.002
Properties after Drying							
untanned	N/A	N/A	N/A	6	370 ± 80	0.12 ± 0.02	0.040 ± 0.005
fully tanned (7 d)	3	2200 ± 700	0.01–0.02	6	1800 ± 300	0.06 ± 0.01	0.018 ± 0.001

<sup>a</sup> ±95% confidence intervals.

parameter was low and the results highly reproducible, making it possible to document a clear distinction between the different kinds of elytra.

Figures 8b and 9b,c show the impact of hydration and tanning on the ratio of viscous modulus  $E''$  to elastic modulus  $E'$ , otherwise known as  $\tan \delta$ , where  $\delta$  is the phase angle between sinusoidally varying stress and strain. The values of this ratio at 1 rad/s are given in Table 3; the trends with tanning time and drying yield a figure quite similar to trends of the frequency exponent  $n$  shown in Figure 10. A high value of this ratio indicates that vibrational damping is high; conversely, a low value indicates highly elastic behavior with minimal energy losses. The untanned elytron exhibits a relatively high  $\tan \delta$  at low frequencies, which sharply declines as a function of frequency. For both species, drying and tanning decrease  $\tan \delta$  and make it less dependent on frequency, though to varying extents. However, the effect of dehydration on  $\tan \delta$  frequency dependence for elytra from both species is substantially different from that of tanning alone or tanning plus drying, suggesting that tanning and drying affect elytral properties to different extents, with the former more predominant. Again, down-regulation of *TcLac2* and *TcADC* both alter  $\tan \delta$  relative to normal elytra but do so quite differently. Decreased *TcADC* expression significantly increases both the magnitude and the frequency dependence of  $\tan \delta$  relative to fully tanned elytra. The same was observed for a natural mutant “black” variant, hypothesized to be ADC-deficient.<sup>58</sup> Knockdown of *TcLac2* transcripts yields elytra after three days quite similar to normal elytra after 24 h, with a relatively high magnitude of  $\tan \delta$  but with less frequency dependence than most other elytral types. The data at higher frequencies are quite noisy because of the small elytral size and relatively low moduli.

## Discussion

**Cuticle Formation in *Tribolium* and *Tenebrio*.** Cuticle physical properties developed in both species of insects in a

similar fashion, consistent with the accepted picture of compositional changes in cuticle over time. Untanned elytra of *Tribolium* and *Tenebrio* are significantly hydrated, soft, and relatively ductile. The stress–strain curves of both untanned and partially tanned elytra generally displayed several local maxima, indicative of piecewise tearing of the untanned cuticle between the ribs. At maturity, the elytra become substantially stiffer with an increase of more than an order of magnitude in the Young’s modulus, while the fracture strain decreases nearly 3-fold. Thus, fully tanned elytra behave as a typical brittle plastic as the stress–strain response is virtually linear to the point of catastrophic failure. Furthermore, the ratio  $E''/E'$  and the frequency exponents drop substantially as a function of tanning time. A low value of this ratio indicates that the material response is predominantly elastic with minimal internal energy losses due to viscous damping. The moduli of untanned and fully tanned elytra of both species are the same within experimental uncertainty, ~50 MPa for untanned and ~1100 MPa for fully tanned. These values are comparable to those measured by Vincent for tanned and untanned cuticles of *Calliphora erythrocephala* maggots.<sup>28,59</sup>

However, tanning proceeds more rapidly in *Tenebrio* than in *Tribolium* (bar charts making the following comparisons are included in Supporting Information). Visually, *Tenebrio* darkens faster than *Tribolium*. The mechanical property data show that after 24 h *Tenebrio*’s moduli have increased on the order of 10 times, while *Tribolium*’s moduli have increased only about 4 times. Furthermore, the frequency exponent  $n$  has dropped more significantly after 24 h in *Tenebrio* than *Tribolium*, indicating increased cross-linking as discussed below. Drying has a much larger impact on the moduli of *Tribolium* than *Tenebrio*, although the fully tanned *Tenebrio* elytron has a somewhat lower frequency exponent, indicating that there could be some underlying differences in the cuticular structures of these insects beyond rate of development.



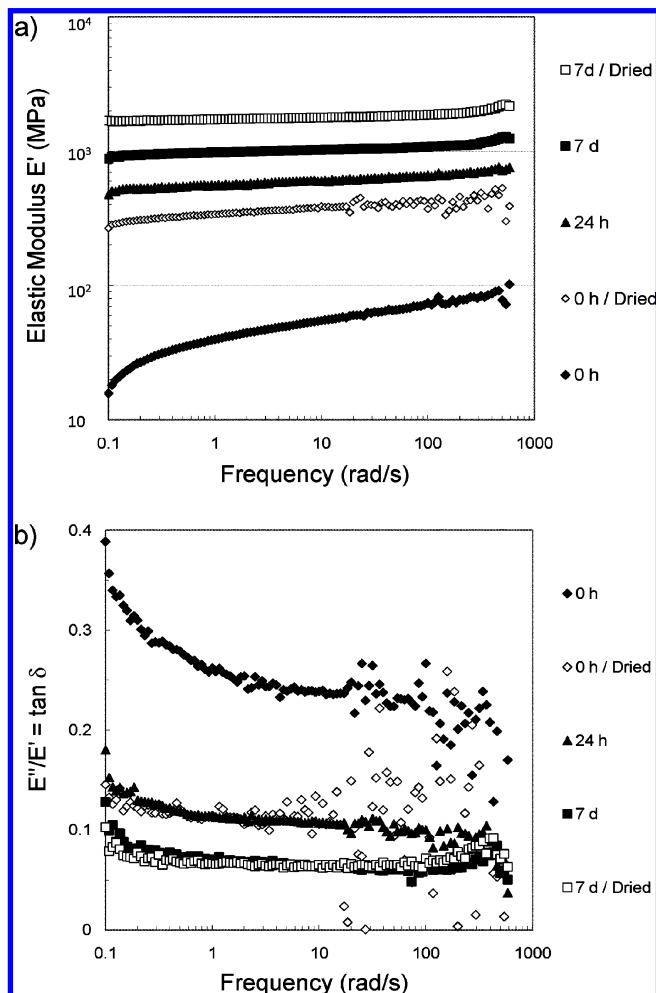


**Figure 8.** (a) Frequency sweep measurement of the elastic modulus at 0.1% strain of *Tenebrio* elytra. The curves are composites of multiple runs, on average four each. The modulus increases 2 orders of magnitude with tanning and the frequency dependence diminishes. Drying of the elytra has a much lesser effect. (b) Frequency sweep measurement of the ratio of the viscous modulus to elastic modulus  $E''/E'$  ( $\tan \delta$ ) at 0.1% strain of *Tenebrio* elytra for the same data sets as in (a). The ratio decreases significantly with tanning and the frequency dependence diminishes. Drying of the elytra has a much lesser effect, especially for the fully tanned cuticle.

It is interesting to note that with tanning and drying toughness increases in *Tenebrio* by a factor of 3 (area under the stress–strain curve). This measure of toughness is formally the work-to-fracture and can also be interpreted as the amount of energy that can be absorbed per unit volume at failure. Because of the irregular nature of the failure, the standard deviation for this property is high. Because brittle failure of a body part leads to a significant loss of function, resistance to failure by the cuticle may be the most significant structural property determining beetle viability over the course of its maturation. In fact, the dsRNA *dsTcLac2* elytra of *Tribolium* have a notably reduced toughness relative to wild-type samples.

Static tensile tests of insect cuticle have been widely reported prior to this report, but such tests are sensitive to sample variation and are thus less reproducible than dynamic mechanical analysis.<sup>27</sup> Torsion pendulum experiments are dynamic mechanical methods that have been applied previously to cuticle in a limited fashion. Similar to our observations, Vincent found that the modulus of maggot cuticle increases an order of magnitude in stiffness upon drying and that tanning affects the slope of the elastic modulus–water content curve.<sup>59</sup> However,

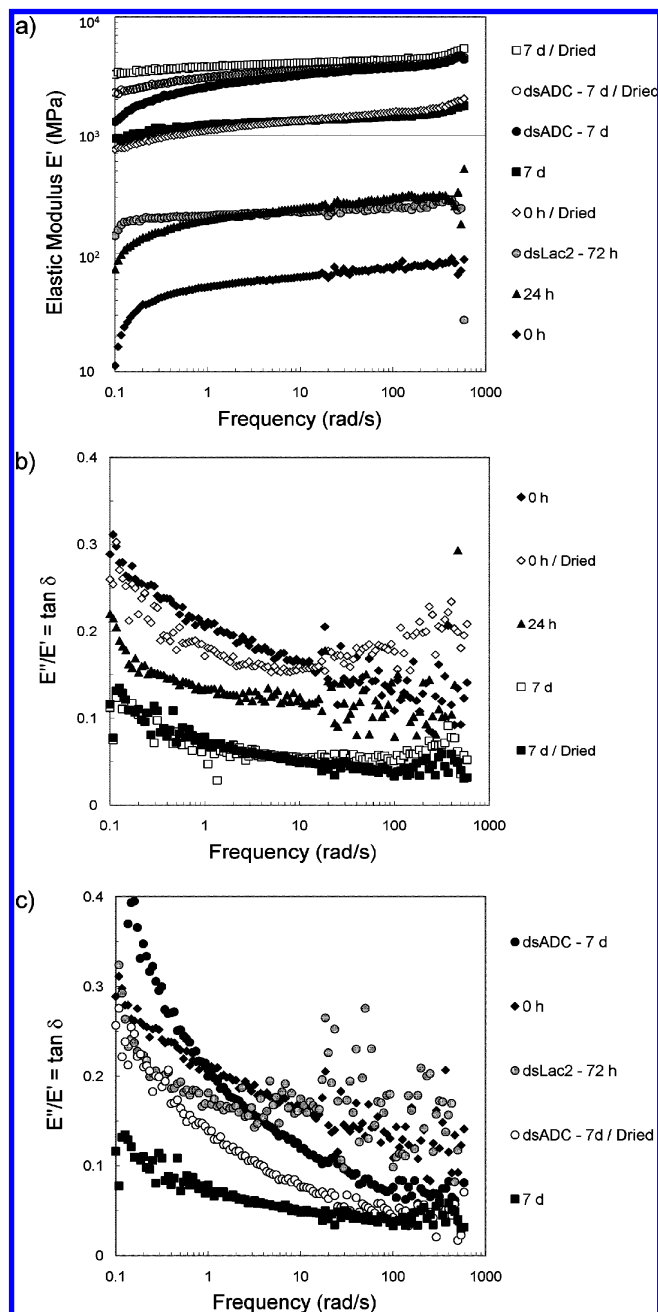


**Figure 9.** (a) Frequency sweep measurement of the elastic modulus at 0.1% strain of *Tribolium* elytra. The behavior is comparable to that of *Tenebrio*. Also shown are the results for elytra in which the enzymes *TcADC* and *TcLac2* in *Tribolium* were suppressed by injection of dsRNA for those genes. Suppression of the enzymes changes the mechanical response of the elytra in very different ways. (b) Frequency sweep measurement of the ratio of the viscous modulus to elastic modulus  $E''/E'$  ( $\tan \delta$ ) at 0.1% strain of *Tribolium* elytra for the same data sets for normally maturing elytra as in (a). The behavior is comparable to that of *Tenebrio*. (c) Frequency sweep measurement of the ratio of the viscous modulus to elastic modulus  $E''/E'$  ( $\tan \delta$ ) at 0.1% strain of *Tribolium* elytra for the same data sets for enzyme-suppressed elytra as in (a); normally tanned elytral data are repeated from Figure 8b for comparison. Suppression of the enzymes changes the mechanical response of the elytra in very different ways. The poor quality of development of the *dsTcLac2* elytra leads to very noisy data above 10 rad/s.

the moduli were not measured as a function of frequency nor was  $E''/E'$  reported to identify the influence of cross-links as was done in this work. Nanoindentation has also been useful for measuring both hardness and stiffness as a function of water

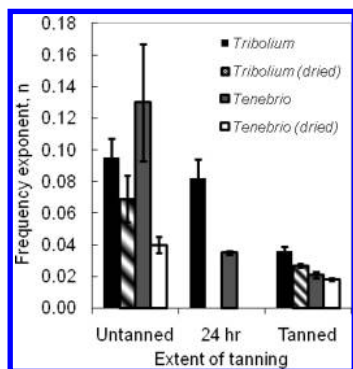


**Figure 10.** Frequency exponents obtained from the elastic moduli data of normally developing elytra in Figures 8a and 9a. The frequency exponents for both species drops more significantly with tanning time than with drying. Similar trends are obtained by comparison of the ratio  $E''/E'$  at 1 rad/s, showing that  $n$  conveys similar information and fits data over a range of frequencies.

content. Barbakadze et al. observed that beetle head articulation cuticle stiffened by an order of magnitude with drying.<sup>60</sup> This method has the advantage of measuring local properties, but it does not provide the same information reflecting intermolecular interactions as DMA. Mechanical testing has also been performed on “cuticle loops” cut from the alloscutum of ticks,<sup>3</sup> but such a method is not generally applicable.

The primary limitations of our method are associated with sample dimensions and gripping. ASTM standards for tensile tests of materials suggest the use of dog-bone shaped samples with a greater length to width ratio than is possible to achieve with these elytra. Such limitations in specimen geometry are a general problem in working with biological specimens and are difficult to eliminate. The elytra are not uniformly thick but taper off toward the ends, so the gripping stresses will also vary laterally in the grips. Thus, end effects caused by stress concentrations at the grips are likely to have been introduced.<sup>61,62</sup> Work on polyethylene films suggests that using these sample dimensions could lead to an underestimate of the true Young’s modulus of the material on the order of a factor of 2.<sup>63,64</sup> Horgan suggests that the end effects would propagate farther into the length of the sample for anisotropic materials.<sup>62,64,65</sup> For biological tissues such as tendon and bone, different results are seen. For tendon, work indicates that the apparent modulus may increase several times with increasing sample length to width ratios.<sup>66</sup> For bone, however, there was a limited effect of dimensions on modulus.<sup>67</sup>

Thus it may be anticipated that the moduli reported in this paper may not be “true” values of the material. However, in the different studies cited above the variations with sample dimension are not more than a factor of two to three at the most. In our work, we get similar results whether cuticle specimens are gripped directly or mounted by epoxy, suggesting that the specific gripping method is not a factor. We saw no significant difference in moduli or frequency dependence when the length to width ratio was changed by a factor of 2 by cutting tanned *Tenebrio* elytra in half lengthwise, whether freshly harvested or dried. Gripping effects have been found not to be substantially different for glassy vs rubbery materials.<sup>68</sup> And as noted above the values obtained in this work are comparable to literature values for insect cuticle obtained by other methods.<sup>5</sup> Therefore, we conclude that despite the possibility of stress concentration artifacts due to the dimensions of the specimens, these effects are not likely to obscure the trends established and conclusions drawn. The approximation of the samples as homogeneous

rectangular slabs and variations in sample dimensions are likely the most substantial sources of deviation of the moduli reported here from their “true” values.

**Evidence of Cross-Linking in Elytral Cuticle.** The results compiled in Table 3 as well as Figures 8a and 9a show that the elastic modulus ( $E'$ ) of the elytron increases by 2 orders of magnitude during tanning, as its water content and chemical composition change simultaneously. It is well-known that solvent softens polymeric materials via plasticization, whereas increased cross-link density stiffens them.<sup>37,51,57,69</sup> In other words, a plasticizing solvent enables polymer chain relaxation, whereas cross-linking inhibits it. That cuticle composition changes during tanning, including conversion of catechols to higher molecular weight hydrophobic pigments like melanin, thus causing dehydration, is well-known.<sup>22,34</sup> Although it has been explained how the reaction of oxidized catechols with cuticular proteins could cross-link these proteins, clear evidence that cross-linking of cuticular solids is a significant contributor to cuticle stiffness in addition to loss of water has been lacking in previous reports on this subject.<sup>28</sup> However, an examination from several perspectives of the dynamic mechanical analysis data obtained in this work offers compelling evidence that cuticle is significantly cross-linked, that cross-linking increases during tanning, and that cross-linking is equally or more important than as dehydration in generating the observed increase in cuticle strength upon tanning.

The dehydration effect is in fact significant, in that drying any type of cuticle does increase its modulus significantly, as is clearly shown in Figures 8a and 9a and Table 3a,b. The elastic moduli of elytral cuticle  $E'$  at 1 Hz increases 20 times upon maturation for both *Tribolium* and *Tenebrio*. Drying does increase the moduli of untanned *Tribolium* elytra a comparable amount to tanning (though the shape of the curve is notably different, the significance of which is discussed below), but the increase upon drying is only 7 times for *Tenebrio*. For fully tanned *Tribolium* elytra, drying increases  $E'$  another 3.3 times, but only 1.8 times in *Tenebrio*. The combination of increased tanning and drying increases the modulus 67 times in *Tribolium* and 35 times in *Tenebrio*.

However, simple comparisons of the magnitude of moduli do not clearly separate the reasons for the differences. It does not determine whether the modulus increase upon drying simply reflects the loss of plasticization or whether dehydration induces development of physical cross-links. Comparisons of moduli do not enable determination of whether changes with tanning time reflect changes in chemical composition (e.g., relative proportions of protein, chitin and catechol) or increases in covalent cross-linking as suggested by the quinone tanning hypothesis. It is undoubtedly true that most of the increased stiffness of the elytra results from changes in chemical composition upon tanning. For example, it is known that melanin is present in some strong biological structures.<sup>70</sup> Thus, the increase in stiffness in itself does not necessarily mean that the tanned elytral cuticle is more cross-linked than the untanned, as the quinone tanning hypothesis suggests.

Frequency sweep analysis, on the other hand, can help to distinguish between cross-linked and uncross-linked materials of similar moduli. Un-cross-linked macromolecular materials resist deformation upon applied stress, but given enough time, they are able to reduce internal stress through polymer chain rearrangements and thus appear softer under lower strain rates.<sup>57,71</sup> However, cross-links limit the movement of polymer chains past one another even over the longest time scales (lowest frequencies). Hence, cross-linked and uncross-linked materials

respond differently to a sinusoidal deformation, especially at low frequencies (at very high frequencies, only side chain or local motions are probed). Most notably, at low frequencies, the elastic modulus  $E'$  of polymers reaches a plateau value if cross-linked, whereas it declines sharply if un-cross-linked. At such frequencies, viscous losses are negligible in cross-linked polymers ( $E''/E'$  can fall below 0.01), whereas they become dominant if un-cross-linked ( $E''/E' > 1$ ).<sup>37</sup> However, for cross-linked polymer networks, the power law frequency exponent  $n$  for  $E'$  is expected to fit over several decades of frequency, declining as cross-linking increases.<sup>41</sup> Since  $n$  is expected to be a strong function of cross-link density but a weak function of solvent content, it should be an important indicator of cross-link formation, even in the presence of dehydration.<sup>72</sup> Some early uses of frequency sweeps of complex biological tissues have observed behavior consistent with this power law behavior, but previously no one has utilized this model to infer internal structure.<sup>73,74</sup> In one case, however, the exponent for this function for entangled biopolymers, specifically actin fibrils, has been reported to be in the range of 0.1 to 0.3.<sup>75</sup>

In fact, all of the tanned elytra tested exhibit only a slight frequency dependence of the elastic modulus  $E'$  for most of the frequency range tested (Figures 8a and 9a). The observation of a limited  $E'$  frequency dependence over multiple decades in this range is consistent with the behavior of synthetic cross-linked polymer networks. Figure 10 shows that the exponents are at the lower range and below the range expected for entangled biopolymers, and approach zero or purely elastic behavior in fully tanned cuticle. For both species, the exponents decline steadily and substantially by more than a factor of 2 with increased tanning, consistent with the process of cross-linking. Drying has no effect on these trends and generally only a small effect in magnitude of the exponents, less than a 40% reduction in all cases except for untanned *Tenebrio* elytra, which declines about 3-fold. These changes might point to the formation of noncovalent cross-links upon drying, though the effect is clearly much less than the effect of tanning time. The fact that dried, untanned *Tribolium* elytra has notably more frequency dependence than freshly harvested (hydrated), fully tanned elytra despite having moduli comparable in magnitude is consistent with untanned elytra having a less cross-linked structure than fully tanned elytra. Thus, examination of the dependence of  $E'$  on frequency points to the development of cross-linking upon tanning of elytra, and that the increase in modulus with tanning involves a different mechanism than the increase seen upon dehydration.

The presence of cross-linking can also be inferred from the frequency dependence of the  $E''/E'$  ratio, which is a measure of viscous damping in the material as a function of tanning and hydration state for both species. Figures 8 and 9 show that, for all elytra, the ratio is much less than 1 (i.e.,  $E' \gg E''$ ), with no more than a modest dependence on frequency. Furthermore, for both species it is quite evident that the ratio declines substantially with tanning time, as does the frequency dependence. Drying has a much smaller effect in both respects, once again demonstrating the insufficiency of dehydration to explain changes in the mechanical properties of cuticle as a function of tanning. Furthermore, these trends also are consistent with the hypothesis of increased cross-linking as tanning proceeds. The decline in the  $E''/E'$  ratio with frequency indicates that increasing frequency causes movement away from a polymer relaxation mode(s) where viscous energy dissipation is relatively high.<sup>37,57</sup> We propose that such modes most likely involve movement of polymer chains past one another. Cross-linking and removal of

a plasticizing solvent will suppress such modes, effectively shifting them to lower frequencies. If that frequency range is below the range measured, cross-linking and drying will be observed as a diminishing frequency dependence of  $E''/E'$ . However, while solvent enables the relaxation modes to occur at a higher frequency, it does not substantially alter them. In contrast, the constraints imposed by cross-linking will be observed as a reduced ratio of  $E''/E'$  at all frequencies where this relaxation mode is active. This behavior suggests that the main effect of drying would be to shift the curve to the left (lower frequencies), while increased cross-linking would also shift it down as well as left. The latter trend is consistent with the data shown in Figures 8b and 9b,c.

It should be noted that the frequency exponent  $n$  and the ratio  $E''/E'$  are different measures of the same phenomena, namely, the combination of viscous and elastic response to applied stresses. Thus, Figure 10 is almost the same if  $E''/E'$  is plotted instead of  $n$  (see Supporting Information for a figure).  $E''/E'$  or  $\tan \delta$  is more widely used than  $n$  as a measure of viscous damping in polymeric materials. However, the choice of frequency to report a particular value of  $E''/E'$  is arbitrary. In contrast, a single value of  $n$  can be extracted and reported from one to two decades or more of frequency data. When used to interpret material behavior, both  $n$  and  $E''/E'$  also have the advantage of being independent of dimension. Because the difficulty in accurately measuring dimensions of these small biological samples is the main source of uncertainty in the reported moduli values, both  $n$  and  $E''/E'$  can be determined much more accurately than moduli. For elytra, we have found  $n$  to be a highly reproducible parameter that is quite sensitive at discriminating among different types of elytra.<sup>48</sup>

These results do not unambiguously distinguish between covalent cross-linking, as suggested by the quinone tanning hypothesis and noncovalent interactions that might be induced, for example, by hydrogen bonding or  $\beta$ -sheet formation among the protein components. For example, in prior work, we have shown that inducing  $\beta$ -sheet formation in poly( $\alpha$ -L-lysine) gels by changing pH can increase the modulus of such networks.<sup>76</sup> However, we believe the fact that increased tanning increases the modulus while substantially decreasing the frequency exponent, whereas dehydration increases the modulus but with a lesser impact on the frequency exponent, supports the hypothesis that tanning increases the cross-linking in the cuticle. We are currently carrying out several lines of inquiry to further separate contributions of covalent and noncovalent cross-linking. One is to extend the frequency sweeps to lower frequencies. It is expected that physical cross-links created by intermolecular hydrogen-bonding would break and reform cooperatively at low time-scales, thus reducing the modulus at low frequencies,<sup>77</sup> while covalent cross-links cannot disengage at any frequency. Our results to date on fully tanned *Tribolium* elytral cuticle show that the modulus remains high, following approximately the same frequency exponent down to 0.001 rad/s, suggesting that cross-links are, in fact, permanent. We are also investigating the mechanical properties of *Tribolium* elytra after treatment with strong hydrogen bond-breaking solvents, such as formic acid. Preliminary results show that although the elytra swell about 30% in formic acid, the Young's modulus does not change significantly. The effects of the formic acid are reversible, as formic acid-swollen, fully tanned elytra subsequently leached of formic acid follow the same frequency sweep profile as untreated elytra. Recent work indicates that reversible plasticization of tick cuticle during feeding is possible by active control of pH in the cuticle, therefore altering hydrogen bonding and



thus water content of the cuticle.<sup>78</sup> Still, even in this specialized form of cuticle, a balance remains between reversible and permanent cross-links. Therefore, the conclusion that covalent cross-links contribute to the mechanical properties of cuticle is supported. However, even these experiments provide no indication of the origin of such cross-links, whether they originate as hypothesized by the quinone tanning hypothesis or by some unrelated reactions. Here we are measuring the properties of intact elytra, which are complex structures, but interpreting the data in terms of the elytral cuticle. In fact, our examination of the tearing phenomena in the static tests suggests that the ribs may tan faster than the cuticle between the ribs, but reach uniform properties upon maturation. However, we believe that our studies using RNAi provide evidence that to a significant extent, the cross-links are of quinone tanning origin, and we will review this evidence in the next section.

**Manipulation of Metabolic Pathways in Cuticle.** The impact of cuticular enzyme-catalyzed reactions during tanning was further illustrated by considering the physical properties of elytra obtained from enzyme-deficient *Tribolium*. Even though the pigmentation and cross-linking developmental pathways are coupled, the ratio of un-cross-linked pigmentation molecules to cross-linked molecules can be affected by altering enzymatic activities.<sup>48</sup> Use of the RNAi technique allowed suppression of the expression of two different enzymes involved in cuticle tanning metabolism, *TcLac2* and *TcADC*. *TcLac2* is a phenoloxidase that has been previously shown to be required in several steps of cuticle tanning (Figure 1).<sup>49</sup> Most notably, it catalyzes the oxidation of catechols, which polymerize to form melanin-based pigments as well as the oxidation of catechols to quinones that subsequently react with cuticular proteins to form adducts and cross-linked proteins. The quinone tanning hypothesis suggests that formation of covalent bonds to proteins can occur multiple times with a single quinone molecule, leading to formation of cross-links. Thus, reducing *Lac2* activity is expected to suppress both formation of pigments and quinone-mediated protein cross-linking. In contrast, *ADC* catalyzes the synthesis of  $\beta$ -alanine used for production of NBAD, a major catecholic cross-linking agent precursor. With reduced *ADC* activity, catechols such as dopamine accumulate and are partitioned more into the pigmentation pathway rather than into the cross-linking pathway.

The RNAi results show that with a partial knockdown of *TcLac2*, light brown elytra develop 72 h post eclosion. The water content is on the order of 50%, slightly less than for untanned elytra ( $54 \pm 5\%$ ) and this phenotype is an order of magnitude weaker ( $E = 230 \pm 140$  MPa) than tanned elytra. In strain sweeps, the elytra begin to break down at lower strains than normally maturing elytra at any stage (Figure 7). The observed lack of coloration, high water content and reduced mechanical strength are consistent with the hypothesis that *dsTcLac2* elytra would have a reduced capability to synthesize hydrophobic structural pigments and to form a cross-linked protein network in the cuticle. Frequency sweep experiments shown in Figure 9a and c further quantify the observed impact of *TcLac2* suppression and help to identify the role of this enzyme in the development of cuticular mechanical properties. At 72 h posteclosion, *TcLac2*-suppressed elytra reach an  $E'$  comparable to that of native elytra at 24 h posteclosion. However, the altered elytra have a lower frequency dependence exponent than both normal untanned and partially tanned elytra. This result indicates that some cross-linking does occur in elytral cuticle when *TcLac2* expression is diminished, but it occurs at a much slower rate. There also is a reduced amount of pigment produced, which

explains the observation of less viscous damping (lower  $E''/E'$ ). Therefore, in *dsTcLac2* elytra, the overall network formation is hindered, in both cross-linked and un-cross-linked cuticular components alike. In terms of rubber elastic theory, though softer due to a diminished cross-link density, *dsTcLac2* elytral cuticle may be a more “perfect” network than normal cuticle because pigmentation components are not present as filler material or that fewer dangling ends of the polymers exist in the altered network.<sup>79</sup>

In contrast to *TcLac2* suppression, *TcADC* suppression in *Tribolium* causes a body color darker than that of wild-type insects, yet the insects were otherwise able to mature normally. The darker color is consistent with the hypothesis that suppressing *ADC* activity would limit L-aspartic acid decarboxylation to  $\beta$ -alanine and conjugation with dopamine to yield NBAD, and thereby enhance the production of melanic pigments from dopamine at the expense of protein cross-linking by quinones derived from NBAD. The expected reduction in protein cross-linking and increase in pigment is supported by the fact that the frequency dependence exponent of *dsTcADC* elytra is greater than that of tanned elytra, also supporting the hypothesis of a greater level of un-cross-linked material relative to cross-linked material in *dsTcADC* elytra (Table 3). A relative deficiency in cross-linking of *dsTcADC* elytral cuticle is further confirmed by the pronounced frequency dependence of  $E''/E'$  (viscous damping), as shown in Figure 9c. Interestingly, the elastic modulus of the *dsTcADC* elytra is several times larger than that for the tanned elytra. This could be the result of an increase in melanin pigmentation, as melanin is known to be associated with hardening in a number of animal structures.<sup>70</sup> It appears that *ADC*-deficient *Tribolium* are able to mature to otherwise normal adults because, while elytra properties were altered, they were adequate for survival, unlike the phenotype from *TcLac2* suppression. We have presented evidence previously that a naturally occurring genetic variant of *Tribolium* called “black” fact a *TcADC*-deficient mutant with a value of  $n$  significantly larger than for other strains.<sup>48,58</sup>

**Potential Applications.** Cuticle can be viewed as an interpenetrating network of chitin embedded in a protein–catechol matrix, and the results of this work are supportive of that view. Recent work by Gong, Osada, and co-workers has demonstrated that a synthetic IPN model system composed of a rigid cross-linked network interpenetrated by a flexible entangled polymer has exceptional mechanical properties compared to the individual networks, even when they are hydrated.<sup>80,81</sup> Because insect cuticle is believed to have a similar organization of its macromolecular components, a better understanding of the origins of the cuticle’s mechanical properties may help to develop technologically significant new materials such as tissue engineering scaffolds for cartilage regeneration. In fact, we have recently demonstrated that interpenetrating networks of agarose and poly(ethylene glycol diacrylate) can be used as scaffolds for chondrocyte encapsulation for cartilage regeneration.<sup>82</sup> The chitin fiber and protein interpenetrating network motif may be useful for the aqueous production of high-performance synthetic composites, avoiding the need, in some cases, for volatile organic solvents to solubilize polymers or reduce viscosity.<sup>83</sup>

This work has also demonstrated that with knowledge of metabolic pathways in the maturation of the cuticle, it is possible to intentionally manipulate the macromolecular structure to either substantially increase or decrease the mechanical performance of that biomaterial. This accomplishment suggests that these methods can be used to exploit the mechanochemistry and molecular-level organization of complex biological struc-

tures like cuticle in order to understand how to engineer properties in composite polymeric networks for applications ranging from aerospace to biomedical implants.<sup>39,84–89</sup> Furthermore, the combination of RNAi and mechanical analysis makes possible systematic exploration of the relative importance of individual components of complex biological composite materials like the insect exoskeleton.

### Conclusions

A comprehensive set of ultimate and dynamic mechanical properties of elytra from *Tribolium* and *Tenebrio* was collected at various tanning stages with particular interest in distinguishing between the contributions of cross-linking and hydration to those properties. The use of two types of beetles of much different sizes validates the testing methods and demonstrates a degree of generality of the results. The two types of mechanical tests used, static (most commonly applied to such biological materials in past studies) and dynamic (most novel characterization method used here), demonstrated both internal consistency of the methods and differences in their utility. The RNAi experiments provided biochemical validation of the hypothesized metabolic pathway believed to account for the changes observed upon tanning.

From the static tests, elytra of freshly ecdysed beetles were shown to behave as soft plastics, which tear under stress to the point of complete failure. When fully tanned, elytral cuticle behaves more like a strong but brittle plastic with properties comparable to engineering polymers such as polystyrene.

Dynamic mechanical analysis showed that, while the water content has an important role in determining cuticle mechanical properties, the tanning reactions themselves contribute substantially to these properties beyond simply inducing dehydration. Elytra, whether tanned or untanned, increase in elastic modulus while drying, but the increase is generally less than observed with tanning itself. Most notably, as tanning time increased, the frequency exponent for  $E'$  approached zero and the ratio of  $E''/E'$  decreased in magnitude while diminishing in frequency dependence. These observations indicate that tanning causes an increase in the elastic component relative to the viscous component of the cuticular network's mechanical response. In contrast, water content has a limited effect on these parameters, as expected, because drying has a limited effect on network topology (e.g., proportion of elastically active network chains).

The evidence for cross-linking in elytral cuticle does not indicate which components of the cuticle are cross-linked or confirm that cross-links are covalent and, thus, does not directly validate the quinone tanning hypothesis for cross-linking of cuticular components. However, the changes observed after injection of dsRNA for *TcLac2* or *TcADC* are consistent with that hypothesis. Reduced ADC activity is hypothesized to increase the amount of pigments relative to cross-linked protein, and this is reflected in a larger viscous component relative to the elastic component of the mechanical response of the cuticle whether hydrated or dried. In contrast, diminished *TcLac2* activity led to a weakened yet relatively elastic cuticle, consistent with a reduction of both total solids and cross-linking, and apparently a greater reduction of the former relative to the latter.

This work also demonstrates the utility of applying dynamic mechanical analysis to help understand the interactions between different components in a complex biological material, a method that is often applied to synthetic polymers but rarely to complex biological materials like cuticle. Other types of cuticle could be tested by this method, whether using instruments of the type

used in this work or nanoindentation systems capable of dynamic mechanical analysis. It also demonstrates the use of RNAi to manipulate metabolic pathways to alter the properties of a biological material in a controlled way to further this understanding. Results obtained with these techniques also indicate that it may be possible to manipulate intentionally the cuticle nanostructure to determine the mechanochemical basis for the structure and to identify key contributors to the observed properties. Such knowledge can be helpful in the design of novel biomimetic technological materials such as tissue engineering scaffolds.

**Acknowledgment.** We thank our colleagues Michael S. Detamore, Anil Misra, Subbaratnam Muthukrishnan, Ranganathan Parthasarathy, and the anonymous reviewers for helpful comments on the manuscript. This material is based on work supported by the National Science Foundation under Grant No. IOS 0726412. Any opinions, findings, and conclusions or recommendations expressed in this article are those of the authors and do not necessarily reflect the views of the National Science Foundation. This is also contribution 08-360-J from the Kansas Agricultural Experiment Station. All programs and services of the U.S. Department of Agriculture are offered on a nondiscriminatory basis, without regard to race, color, national origin, religion, sex, age, marital status, or handicap.

**Supporting Information Available.** Additional material on the physical, static mechanical, and dynamic mechanical properties is available. Scanning electron micrographs of elytra are provided. The data in Tables 1–3 are presented as bar charts to illustrate the trends. Additional data demonstrating the reproducibility and consistency of mechanical test methods used is provided. This material is available free of charge via the Internet at <http://pubs.acs.org>.

### References and Notes

- (1) Lakes, R. *Viscoelastic Materials*; Cambridge University Press: Cambridge, U.K., 2009.
- (2) Neville, A. C. *The Biology of the Arthropod Cuticle*; Springer-Verlag: New York, NY, 1975.
- (3) Moussian, B. Recent advances in understanding mechanisms of insect cuticle differentiation. *Insect Biochem. Mol. Biol.* **2010**, *40* (5), 363–375.
- (4) Wegst, U. G. K.; Ashby, M. F. The mechanical efficiency of natural materials. *Philos. Mag.* **2004**, *84* (21), 2167–2186.
- (5) Vincent, J. F. V.; Wegst, U. G. K. Design and mechanical properties of insect cuticle. *Arthropod Struct. Dev.* **2004**, *33* (3), 187–199.
- (6) Cribb, B. W.; Stewart, A.; Huang, H.; Truss, R.; Noller, B.; Rasch, R.; Zalucki, M. P. Insect mandibles-comparative mechanical properties and links with metal incorporation. *Naturwissenschaften* **2008**, *95* (1), 17–23.
- (7) Schoberl, T.; Jager, I. L. Wet or dry: Hardness, stiffness and wear resistance of biological materials on the micron scale. *Adv. Eng. Mater.* **2006**, *8* (11), 1164–1169.
- (8) Vincent, J. F. V.; Shawky, N. A. F. The proteins of the urea-soluble fraction of locust intersegmental membrane. *Insect Biochem.* **1978**, *8* (4), 255–261.
- (9) Miserez, A.; Schneberk, T.; Sun, C.; Zok, F. W.; Waite, J. H. The transition from stiff to compliant materials in squid beaks. *Science* **2008**, *319*, 1816–1819.
- (10) Miserez, A.; Rubin, D.; Waite, J. H., Cross-linking chemistry of squid beak. *J. Biol. Chem.* **2010**, *285* (49), 38115–38124.
- (11) Orso, S.; Wegst, U.; Eberl, C.; Arzt, E. Micrometer-scale tensile testing of biological attachment devices. *Adv. Mater.* **2006**, *18* (7), 874–877.
- (12) Wegst, U. G. K. *Natural Materials Selector, created using the CES Construction Software*; Granta Design Ltd.: Cambridge, U.K., 2004.
- (13) Chen, J.; Ni, Q. Q.; Xu, Y.; Iwamoto, M. Lightweight composite structures in the forewings of beetles. *Compos. Struct.* **2007**, *79* (3), 331–337.
- (14) Chen, J.; Dai, G.; Xu, Y.; Iwamoto, M. Optimal composite structures in the forewings of beetles. *Compos. Struct.* **2007**, *81*, 432–437.

- (15) Hepburn, H. R.; Farr, J. M. On the structure of the cuticle of *Mecoptera*. *J. Entomol.* **1975**, *50A*, 97–105.
- (16) Lehane, M. J. Peritrophic matrix structure and function. *Ann. Rev. Entomol.* **1997**, *42* (1), 525–550.
- (17) Rebers, J. E.; Riddiford, L. M. Structure and expression of a *Manduca sexta* larval cuticle gene homologous to *Drosophila* cuticle genes. *J. Mol. Biol.* **1988**, *203* (2), 411–423.
- (18) Rebers, J. E.; Willis, J. H. A conserved domain in arthropod cuticular proteins binds chitin. *Insect Biochem. Mol. Biol.* **2001**, *31* (11), 1083–1093.
- (19) Sugumaran, M. Unified mechanism for sclerotization of insect cuticle. *Adv. Insect Physiol.* **1998**, *27*, 229–334.
- (20) Kramer, K. J.; Kanost, M. R.; Hopkins, T. L.; Jiang, H.; Zhu, Y. C.; Xu, R.; Kerwin, J. L.; Turecek, F. Oxidative conjugation of catechols with proteins in insect skeletal systems. *Tetrahedron* **2001**, *57* (2), 385–392.
- (21) Pryor, M. G. M. On the hardening of the ootheca of *Blatta orientalis*. *Proc. R. Soc. B* **1940**, *128* (852), 378–393.
- (22) Andersen, S. O. Cuticular sclerotization and tanning. In *Comprehensive Molecular Insect Science*; Gilbert, L. I., Iatrou, K., Gill, S., Eds.; Elsevier: Oxford, U.K., 2005; Vol. 4, pp 145–170.
- (23) Miserez, A.; Li, Y.; Waite, J. H.; Zok, F. Jumbo squid beaks: Inspiration for design of robust organic composites. *Acta Biomater.* **2007**, *3* (1), 139–149.
- (24) Schaefer, J.; Kramer, K. J.; Garbow, J. R.; Jacob, G. S.; Stejskal, E. O.; Hopkins, T. L.; Speirs, R. D. Aromatic cross-links in insect cuticle: detection by solid-state <sup>13</sup>C and <sup>15</sup>N NMR. *Science* **1987**, *235* (4793), 1200–1204.
- (25) Kerwin, J. L.; Whitney, D. L.; Sheikh, A. Mass spectrometric profiling of glucosamine, glucosamine polymers and their catecholamine adducts. Model reactions and cuticular hydrolysates of *Toxorhynchites amboinensis* (Culicidae) pupae. *Insect Biochem. Mol. Biol.* **1999**, *29* (7), 599–607.
- (26) Suderman, R. Cuticle sclerotization in *Manduca sexta*: an in vitro sclerotization model. Ph.D. Biochemistry, Kansas State University, Manhattan, KS, 2004.
- (27) Vincent, J. F. V.; Hillerton, J. E. The tanning of insect cuticle—A critical review and a revised mechanism. *J. Insect Physiol.* **1979**, *25* (8), 653–658.
- (28) Vincent, J. F. V. If it's tanned it must be dry: A critique. *J. Adhes.* **2009**, *85* (11), 755–769.
- (29) Andersen, S. O. The stabilization of locust cuticle. *J. Insect Physiol.* **1981**, *27* (6), 393–396.
- (30) Gehrke, S. H. Synthesis and properties of hydrogels used for drug delivery. In *Transport Processes in Pharmaceutical Systems*; Amidon, G. L., Lee, P. I., Topp, E. M., Eds.; Marcel Dekker, Inc.: New York, NY, 2000; pp 473–546.
- (31) Treloar, L. R. G. *The Physics of Rubber Elasticity*, 3rd ed.; Clarendon Press: Oxford, U.K., 1975.
- (32) Zhang, X.; Do, M. D.; Casey, P.; Sulistio, A.; Qiao, G. G.; Lundin, L.; Lillford, P.; Kosaraju, S. Chemical cross-linking gelatin with natural phenolic compounds as studied by high-resolution NMR spectroscopy. *Biomacromolecules* **2010**, *11* (4), 1125–1132.
- (33) Sun, S. M.; Mitchell, J. R.; MacNaughtan, W.; Foster, T. J.; Harabagiu, V.; Song, Y. H.; Zheng, Q. Comparison of the mechanical properties of cellulose and starch films. *Biomacromolecules* **2010**, *11* (1), 126–132.
- (34) Andersen, S. O.; Peter, M. G.; Roepstorff, P. Cuticular sclerotization in insects. *Comp. Biochem. Physiol., Part B: Biochem. Mol. Biol.* **1996**, *113* (4), 689–705.
- (35) Andersen, S. O.; Rafn, K.; Krogh, T. N.; Hojrup, P.; Roepstorff, P. Comparison of larval and pupal cuticular proteins in *Tenebrio molitor*. *Insect Biochem. Mol. Biol.* **1995**, *25* (2), 177–187.
- (36) Snider, G. R.; Lomakin, J.; Singh, M.; Gehrke, S. H.; Detamore, M. S. Regional dynamic tensile properties of the TMJ disc. *J. Dental Res.* **2008**, *87* (11), 1053–1057.
- (37) Ferry, J. D. *Viscoelastic Properties of Polymers*, 3rd ed.; John Wiley & Sons, Inc.: New York, NY, 1980.
- (38) Hess, W.; Vilgis, T. A.; Winter, H. H. Dynamical critical-behavior during chemical gelation and vulcanization. *Macromolecules* **1988**, *21* (8), 2536–2542.
- (39) Kim, H.; Macosko, C. W. Morphology and properties of polyester/exfoliated graphite nanocomposites. *Macromolecules* **2008**, *41* (9), 3317–3327.
- (40) Kong, H. J.; Wong, E.; Mooney, D. J. Independent control of rigidity and toughness of polymeric hydrogels. *Macromolecules* **2003**, *36* (12), 4582–4588.
- (41) Mani, S.; Winter, H. H.; Silverstein, M.; Narkis, M. Power law relaxation in an interpenetrating polymer network. *Colloid Polym. Sci.* **1989**, *267* (11), 1002–1006.
- (42) Morse, D. C. Viscoelasticity of concentrated isotropic solutions of semiflexible polymers. 2. Linear response. *Macromolecules* **1998**, *31* (20), 7044–7067.
- (43) Schwittay, C.; Mours, M.; Winter, H. H. Rheological expression of physical gelation in polymers. *Faraday Discuss.* **1995**, 93–104.
- (44) Wachsstock, D. H.; Schwarz, W. H.; Pollard, T. D. Cross-linker dynamics determine the mechanical properties of actin gels. *Biophys. J.* **1994**, *66*, 801–809.
- (45) Richards, S.; Gibbs, R. A.; Weinstock, G. M.; Brown, S. J.; Denell, R.; Beeman, R. W.; Bucher, G.; Friedrich, M.; Grimmelikhuijzen, C. J. P.; Klingler, M.; Lorenzen, M.; Roth, S.; Schroder, R.; Tautz, D.; Zdobnov, E. M. The genome of the model beetle and pest *Tribolium castaneum*. *Nature* **2008**, *452* (7190), 949–955.
- (46) Tomoyasu, Y.; Denell, R. E. Larval RNAi in *Tribolium* (Coleoptera) for analyzing adult development. *Dev. Genes Evol.* **2004**, *214* (11), 575–578.
- (47) Tomoyasu, Y.; Miller, S. C.; Tomita, S.; Schoppmeier, M.; Grossmann, D.; Bucher, G. Exploring systemic RNA interference in insects: a genome-wide survey for RNAi genes in *Tribolium*. *Genome Biol.* **2008**, *9* (1), R10.1R10.22.
- (48) Arakane, Y.; Lomakin, J.; Beeman, R. W.; Muthukrishnan, S.; Gehrke, S. H.; Kanost, M. R.; Kramer, K. J. Molecular and functional analyses of amino acid decarboxylases involved in cuticle tanning in *Tribolium castaneum*. *J. Biol. Chem.* **2009**, *284* (24), 16584–16594.
- (49) Arakane, Y.; Muthukrishnan, S.; Beeman, R. W. T.; Kanost, M.; Kramer, K. J. Laccase 2 is the phenoloxidase gene required for beetle cuticle tanning. *Proc. Natl. Acad. Sci. U.S.A.* **2005**, *102* (32), 11337–11342.
- (50) Arakane, Y.; Muthukrishnan, S.; Kramer, K. J.; Specht, C. A.; Tomoyasu, Y.; Lorenzen, M. D.; Kanost, M.; Beeman, R. W. The *Tribolium* chitin synthase genes *TcCHS1* and *TcCHS2* are specialized for synthesis of epidermal cuticle and midgut peritrophic matrix. *Insect Mol. Biol.* **2005**, *14* (5), 453–463.
- (51) Macosko, C. W. *Rheology: Principles, Measurements, and Applications*; Wiley-VCH: New York, NY, 1994.
- (52) Hopkins, T. L.; Morgan, T. D.; Kramer, K. J. Catecholamines in hemolymph and cuticle during larval, pupal, and adult development of *Manduca sexta* (L). *Insect Biochem.* **1984**, *14* (5), 533–540.
- (53) Roseland, C. R.; Kramer, K. J. Cuticular strength and pigmentation of rust-red and black strains of *Tribolium castaneum*: correlation with catecholamine and  $\alpha$ -alanine content. *Insect Biochem.* **1987**, *17* (1), 21–28.
- (54) Andersen, S. O.; Roepstorff, P. Aspects of cuticular sclerotization in the locust *Scistocerca gregaria*, and the beetle, *Tenebrio molitor*. *Insect Biochem. Mol. Biol.* **2007**, *37* (3), 223–234.
- (55) Sperling, L. H. *Introduction to Physical Polymer Science*, 4th ed.; Wiley: New York, 2004.
- (56) Hillerton, J. E. Cuticle: Mechanical Properties. In *Biology of the Integument*; Bereiter-Hahn, J., Matoltsy, A. G., Richards, K. S., Eds. 1984; Vol. 1, pp 622–637.
- (57) Fried, J. R. *Polymer Science and Technology*, 2nd ed.; Prentice Hall: Upper Saddle River, NJ, 2003.
- (58) Lomakin, J.; Arakane, Y.; Kramer, K. J.; Beeman, R. W.; Kanost, M. R.; Gehrke, S. H. Mechanical properties of elytra from *Tribolium castaneum* wild-type and body color mutant strains. *J. Insect Physiol.* **2010**, *56*, 1901–1906.
- (59) Vincent, J. F. V. Dynamics of drying in phenolically tanned materials. *J. Bionic Eng.* **2004**, *1* (1), 4–8.
- (60) Barbakadze, N.; Enders, S.; Gorb, S.; Arzt, E. Local mechanical properties of the head articulation cuticle in the beetle *Pachnoda marginata* (Coleoptera, Scarabaeidae). *J. Exp. Biol.* **2006**, *209* (4), 722–730.
- (61) Young, W. C.; Budynas, R. G. *Roark's Formulas for Stress and Strain*; McGraw-Hill: New York, 1989.
- (62) Ward, I.; Sweeney, J. *The Mechanical Properties of Solid Polymers*, 2nd ed.; John Wiley & Sons Ltd.: Chichester, West Sussex, England, 2004.
- (63) Lewis, E. L. V. An experimental study of end effects in the extensional deformation of polymers. *J. Mater. Sci.* **1979**, *14* (10), 2343–2352.
- (64) Arridge, R. G. C.; Folkes, M. J. Effect of sample geometry on the measurement of mechanical properties of anisotropic materials. *Polymer* **1976**, *17* (6), 495–500.
- (65) Horgan, C.; Simmonds, J. Saint-Venant end effects in composite structures. *Composites Eng.* **1994**, *4* (3), 279–286.
- (66) Legerlotz, K.; Riley, G. P.; Screen, H. R. C. Specimen dimensions influence the measurement of material properties in tendon fascicles. *J. Biomech.* **2010**, *43*, 2274–2280.



- (67) Lievers, W.; Waldman, S.; Pilkey, A. Minimizing specimen length in elastic testing of end-constrained cancellous bone. *J. Mech. Behav. Biomed. Mater.* **2010**, *3*, 22–30.
- (68) Makke, A.; Perez, M.; Lame, O.; Barrat, J.-L. Mechanical testing of glassy and rubbery polymers in numerical simulations: Role of boundary conditions in tensile stress experiments. *J. Chem. Phys.* **2009**, *131*, 014904–1-014904–8.
- (69) Menard, K. P. *Dynamic Mechanical Analysis: A Practical Introduction*; CRC Press: Boca Raton, FL, 1999.
- (70) Moses, D. N.; Harreld, J. H.; Stucky, G. D.; Waite, J. H. Melanin and glyceric acids—Emerging dark side of a robust biocomposite structure. *J. Biol. Chem.* **2006**, *281* (46), 34826–34832.
- (71) Rosen, S. L. *Fundamental Principles of Polymeric Materials*, 2nd ed.; John Wiley and Sons: New York, NY, 1993.
- (72) Scanlan, J. C.; Winter, H. H. Composition dependence of the viscoelasticity of end-linked poly(dimethyl siloxane) at the gel point. *Macromolecules* **1991**, *24* (1), 47–54.
- (73) Gosline, J. M. Connective tissue mechanics of *Metridium senile*: II. Visco-elastic properties and macromolecular model. *J. Exp. Biol.* **1971**, *55* (3), 775–795.
- (74) Reynolds, S. E. Mechanical properties of abdominal cuticle of *Rhodnius* larvae. *J. Exp. Biol.* **1975**, *62* (1), 69–80.
- (75) Hoffman, B. D.; Massiera, G.; Crocker, J. C. Forced unfolding of protein domains determines cytoskeletal rheology. <http://arxiv.org/abs/physics/0504051>, 2005.
- (76) Oliveira, E. D.; Hirsch, S. G.; Spontak, R. J.; Gehrke, S. H. Influence of polymer conformation on the shear modulus and morphology of polyallylamine and poly( $\alpha$ -L-lysine) hydrogels. *Macromolecules* **2003**, *36* (16), 6189–6201.
- (77) Nissan, A. H. H-bond dissociation in hydrogen bond dominated solids. *Macromolecules* **1976**, *9* (5), 840–850.
- (78) Kaufman, W. B.; Flynn, P. C.; Reynolds, S. E. Cuticular plasticization in the tick *Amblyomma hebraeum* (Acari: Ixodidae): possible roles of monoamines and cuticular pH. *J. Exp. Biol.* **2010**, *213* (16), 2820–2831.
- (79) Rubinstein, M.; Colby, R. H. *Polymer Physics*; Oxford University Press, U.S.A.: New York, NY, 2003.
- (80) Gong, J. P.; Katsuyama, Y.; Kurokawa, T.; Osada, Y. Double-network hydrogels with extremely high mechanical strength. *Adv. Mater.* **2003**, *15* (14), 1155–1158.
- (81) Na, Y. H.; Kurokawa, T.; Katsuyama, Y.; Tsukeshiba, H.; Gong, J. P.; Osada, Y.; Okabe, S.; Karino, T.; Shibayama, M. Structural characteristics of double network gels with extremely high mechanical strength. *Macromolecules* **2004**, *37* (14), 5370–5374.
- (82) DeKosky, B. J.; Ingavle, G.; Dormer, N.; Roatch, C. R.; Lomakin, J.; Detamore, M. S.; Gehrke, S. H. Hierarchically designed agarose and poly(ethylene glycol) interpenetrating network hydrogels for cartilage tissue engineering. *Tissue Eng., C* **2010**, *16* (6), 1533–1542.
- (83) Long, A. C. *Composites Forming Technologies*; Woodhead: Cambridge, U.K., 2007.
- (84) Lee, K. Y.; Mooney, D. J. Hydrogels for tissue engineering. *Chem. Rev.* **2001**, *101* (7), 1869–1880.
- (85) Durmus, A.; Kasgoz, A.; Macosko, C. W. Mechanical properties of linear low-density polyethylene (LLDPE)/clay nanocomposites: Estimation of aspect ratio and interfacial strength by composite models. *J. Macromol. Sci., Part B* **2008**, *47* (3), 608–619.
- (86) Pines, D. J.; Bohorquez, F. Challenges facing future micro-air-vehicle development. *J. Aircraft* **2006**, *43* (2), 290–305.
- (87) Miessner, M.; Peter, M. G.; Vincent, J. F. V. Preparation of insect-cuticle-like biomimetic materials. *Biomacromolecules* **2001**, *2* (2), 369–372.
- (88) Vincent, J. F. V. Arthropod cuticle: a natural composite shell system. *Composites, Part A* **2002**, *33* (10), 1311–1315.
- (89) Qin, G.; Lapidot, S.; Numata, K.; Hu, X.; Meirovitch, S.; Dekel, M.; Podoler, I.; Shoseyov, O.; Kaplan, D. L. Expression, cross-linking, and characterization of recombinant chitin binding resilin. *Biomacromolecules* **2009**, *10*, 3227–3234.

BM1009156